HOKKAIDO UNIVERSITY

Title	A Study on High-Speed Calculation using the Characteristics of Human Eyes in Computer-Generated Hologram
Author(s)	韋, 霊傑
Degree Grantor	北海道大学
Degree Name	博士(情報科学)
Dissertation Number	甲第14284号
Issue Date	2020-09-25
DOI	https://doi.org/10.14943/doctoral.k14284
Doc URL	https://hdl.handle.net/2115/79600
Type	doctoral thesis
File Information	Lingjie_Wei.pdf

Hokkaido University Collection of Scholarly and Academic Papers : HUSCAP



HOKKAIDO UNIVERSITY

A Study on High-Speed Calculation using the Characteristics of Human Eyes in Computer-Generated Hologram

a dissertation presented
by
LINGJIE WEI
to
Graduate School of Information Science and Technology

in partial fulfillment of the requirements
for the degree of
Ph.D of Information Science and Technology
in the field of
Media and Network Technology

Hokkaido University
Sapporo, Hokkaido
August 2020

Contents

1 Introduction **1**
- 1.1 3D visual factors of human eyes . . . 3
- 1.2 The present and future of 3D technology . . . 5
  - 1.2.1 3D technology at present . . . 5
    - 1.2.1.1 Glasses-type 3D technology . . . 5
    - 1.2.1.2 Naked-eye 3D technology . . . 7
  - 1.2.2 3D technology in the future . . . 8
- 1.3 The background of this thesis . . . 11
- 1.4 The purpose of this thesis . . . 12
- 1.5 The structure of this thesis . . . 14

2 Holography **15**
- 2.1 The concept of holography . . . 17
  - 2.1.1 The recording part of holography . . . 18
  - 2.1.2 The reconstruction part of holography . . . 20
- 2.2 The Computer-generated Hologram . . . 21
  - 2.2.1 Various advantages and disadvantages of CGH . . . 21
  - 2.2.2 Various calculation methods for CGH . . . 23
  - 2.2.3 The point-based method . . . 25
  - 2.2.4 The ray-tracing method . . . 28
- 2.3 Digital holography . . . 30

3 The fourier transform optical system **32**
- 3.1 The concept and structure of FTOS . . . 33
- 3.2 Point light source position correction based on FTOS . . . 35

4 Foveated rendering **38**
- 4.1 The concept of foveated rendering . . . 38
- 4.2 Visual acuity . . . 40

4.3 Some conventional methods using foveated rendering 42

5 CGH high-speed calculation using foveated rendering **44**
5.1 Overview of the proposed method using foveated rendering 45
5.2 CGH resolution based on Fresnel zone plate 46
5.3 The luminance of point light sources based on Fresnel zone plate 50
5.4 CGH fast calculation with foveated rendering 51
5.5 Experiments and results for CGH with foveated rendering 54
5.5.1 Experimental environment and devices for CGH with foveated rendering 54
5.5.2 Experiment and results for CGH resolution 54
5.5.3 Experiment and results for luminance 56
5.5.4 Experiment and results for the calculation time 60
5.5.5 Subjective experiment and results 61
5.5.6 Conclusion for the CGH with foveated rendering 66

6 Saccade **68**
6.1 The concept of saccade 68
6.2 Some applications of saccade suppression 71

7 CGH high-speed calculation using saccade suppression **73**
7.1 Overview of the proposed method using saccade suppression 74
7.2 Human reaction time 76
7.3 Duration time of saccade suppression 77
7.4 High-speed calculation of CGH based on saccade suppression 79
7.5 Experiments and results for CGH with saccade suppression 81
7.5.1 Experimental environment and devices for CGH with saccade suppression 81
7.5.2 Design of the subjective experiments 82
7.5.3 Results for the subjective experiment 87
7.5.4 Results for the calculation time 92
7.5.5 Conclusion for the CGH with saccade suppression 94

8 Discussion and summary **96**

References **103**

Listing of figures

2.1 The recording part of holography 19
2.2 The reconstruction part of holography 20
2.3 The compare of traditional optical holography and CGH 24
2.4 The point-based method 27
2.5 The ray-tracing method 29

3.1 The structure of FTOS 33
3.2 The expansion of field of view by FTOS 34
3.3 The position correction for FTOS 36

4.1 Eye structure 41

5.1 Reduce the ray number by expanding the ray angle 47
5.2 Example of snowman 47
5.3 The relationship between zone plate and resolution limit 49
5.4 Holographic display for CGH with foveated rendering 55
5.5 CGH reconstruction image without changing the radius of zone plate . . 57
5.6 Reconstruction images with different radius of Fresnel zone plate 57
5.7 Relationship between CGH resolution and radius of Fresnel zone plate . 58
5.8 Luminance changed with the area of Fresnel zone plate 59
5.9 Luminance corrected pattern of CGH 60
5.10 Calculation time of each foveated quality compared with non-foveated rendering 62
5.11 Calculation speed in wider field of view 63
5.12 Sample of reconstruction images 65
5.13 Average MOS of characters A, B, and C 66

6.1 Conceptual figure of saccade suppression 70

7.1 CGH fast calculation with saccade suppression 75

7.2 CGH fast calculation with saccade suppression and reaction time 77
7.3 The relationship between duration time of saccade suppression and amplitude angle of human eye 78
7.4 Expand the ray angle 80
7.5 Reduce the radius of Fresnel zone plate 80
7.6 Holographic device for CGH with saccade suppression in concept . . . 83
7.7 Holographic device for CGH with saccade suppression in real 84
7.8 Example of the jumping motion of object 85
7.9 Example of the patterns and reconstruction images of reducing CGH resolution 86
7.10 Movement of the object in different types of CGH animations 88
7.11 Part of results of the saccade 90
7.12 Evaluation result in average 91
7.13 Calculation time of Character A 93
7.14 Calculation speed 94

List of Tables

5.1 Parameters of computer for CGH with foveated rendering 54
5.2 Parameters of holographic display for CGH with foveated rendering . . 55
5.3 MOS evaluation 64

7.1 Parameters of computer for CGH with saccade suppression 82
7.2 Parameters of holographic display for CGH with saccade suppression . 82
7.3 Details about the evaluation 87
7.4 Results of t-Test 92

1

Introduction

CG was originally the abbreviation of Computer Graphics. It is a general term for all graphics drawn through computer software. Generally speaking, the computer graphics refers to the following things academically:

- Use a computer to express or process image datas
- Various kinds of techniques for creating or processing image datas

- For the study of digital synthesis and processing of visual content in the field of computer science

With the formation of a series of related industries that use computer as the main tool for visual design and production, the field of visual design and production using computer technology is commonly known as CG. It includes both technology and art, including almost all the visual art creation activities in the current computer era, such as the design of prints [1], web design [2], 3D animation [3], 3D games [4], 3D TVs [5], film and television special effects [6], virtual reality technology [7], multimedia technology [8], architectural design based on computer-aided design [9] and industrial modeling design [10], etc. Nowadays, computers and computer-generated images touch multiple levels of daily life and computer images appears everywhere in our world. [11] can make us easily understand the developing of CG.

Computer Animation is a technology that uses computers to create animations. It can be roughly divided into two types: two-dimensional animation (2D Animation) and three-dimensional animation (3D Animation). Today's CG field has developed many powerful tools to make data more visual and user-friendly. With the continuous development of CG technology, 3D computer graphics technology has become more and more mature, but 2D computer graphics technology is still being widely used. In this short period of more than ten years, CG has relied on high-end science and technology, and unlimited creativity as content, which has completely overturned the traditional visual era and opened up a new era of colorful images. CG animation has brought power to film and game and game powers nearly 100 billion US dollars in economic profits. It can be said that CG has formed an industry all over the world, which profoundly affects

our economic and cultural development.

1.1 3D visual factors of human eyes

3D is short for "Three Dimensions" and refers to three dimensions and three coordinates, namely length, width and height. Today's 3D mainly refers to digital 3D based on computers and the Internet, three-dimensional technology, that is, three-dimensional digitalization. Including 3D software technology and hardware technology.

For human beings, there is usually a distance of a few centimeters between the two eyes of a person, and 3D imaging is generated by the visual difference of these two centimeters of the two eyes. In order for people to see 3D images, it is necessary to allow the left and right eyes to see different images, so that there is a certain gap between the two screens, which is to simulate the actual human eye when watching. This is how the 3D stereoscopic feeling comes from. When the human eye perceives three-dimensional objects, it mainly consists of the following factors:

- binocular parallax
- motion parallax
- accommodation
- convergence

Binocular parallax is due to the distance between the two eyes of the person (the average is 65mm), so for the same scene, the relative positions of the left and right eyes are different, which produces binocular parallax, that is, the left and right eyes see different image.

Motion parallax is caused by the relative movement of the observer and the scene. This movement changes the projection of the scene's size and position on the retina, resulting in a sense of depth. When looking at a fixed object with one eye, the adjustment becomes the only effective hint to the sense of depth. However, if the viewing position is allowed to move, we can use the effect of binocular parallax to view objects from all directions. This effect is called motion parallax. It is particularly important when the viewer moves quite fast, such as sitting on an airplane or an extremely fast train.

Accommodation means the adaptive adjustment of the human eye refers to the active focusing behavior of the eye. The focal length of the eye can be finely adjusted by the lens in its internal structure. The change in focal length allows us to see clearly different sceneries and different parts of the same scene. In general, the minimum focal length of the human eye is 1.7cm, and there is no upper limit. The adjustment of the lens is achieved through the contraction and relaxation of the attached muscles. The movement information of the muscles is fed back to the brain to help establish the three-dimensional sense. Even if we look at an object with one eye, this three-dimensional sense is still there, so it can be said to be a monocular depth hint. However, this kind of hint is only effective when combined with other binocular hints, and the viewing distance is within 2m.

Convergence means when the two eyes look at a point on the object, the visual axes of the two eyes will converge. The angle between the two visual axes is called the convergence angle. For different object points in space, the visual axis will change. In order to achieve this convergence, the human eye muscles need to pull the eyeball to rotate. When the muscle activity is fed back to the human brain, it will give a sense of

depth. Experiments show that there is an interaction between adaptive adjustment and convergence. On the one hand, the convergence information corresponding to a certain distance automatically causes a certain degree of adjustment. On the other hand, the adjusted information also affects convergence. This effect can be proved by a simple experiment, that is, we cover one eye and move the object that the other eye is looking at. When the distance of the object suddenly changes from infinity to 20 cm, it will take 0.2s to 0.3s to response the adjustment with the given distance information.

1.2 The present and future of 3D technology

1.2.1 3D technology at present

3D technology can be traced back to the 19th century. In 1838, the British physicist Charles Wheatstone invented the stereoscope, which is the earliest device that can watch 3D stereoscopic images. His device seems complicated and large but it is very effective. Only through the mirrors with 45 degrees inclination on both sides and the pictures placed on both sides, when the human eye looks directly at the mirror from the front, the same object seen by both eyes is different, which produces a three-dimensional stereoscopic visual experience, thus opening up people's 3D visual experience. At present, 3D display technology can be divided into two categories: glasses type and naked-eye type.

1.2.1.1 Glasses-type 3D technology

In the field of consumption, whether it is a display, a projector or a TV, it is necessary to use it with 3D glasses. For glasses-type 3D technology, we can subdivide three types:

color difference type [12], polarized type [13] and active shutter type [14], which is commonly called color division method, light division method and time division method.

Color difference type galsses uses Anaglyphic 3D technology in conjunction with passive red-blue (or red-green, red-cyan) filter 3D glasses. This technology has the longest history, simple imaging principle, and relatively low implementation cost. The cost of glasses is only a few dollars, but the 3D picture effect is also the worst. Color difference 3D first divides the spectral information by the rotating filter wheel, and uses different color filters to filter the picture, so that one picture can produce two images, and each eye of the person sees a different image. Such a method is easy to cause color cast on the edge of the screen. Due to the poor effect, color-difference 3D technology is not widely used.

Polarized type galsses uses Polarized 3D technology with the principle of "vibration direction" of light to decompose the original image. First, the image is divided into two groups of vertically polarized light and horizontally polarized light, and then the left and right of the 3D glasses use polarized lenses with different polarization directions In this way, the human left and right eyes can receive two sets of images, and then synthesize stereoscopic images through the brain. Among the polarized 3D systems, the more mainstream ones in the market are IMAX 3D, RealD 3D, and MasterImage 3D. IMAX 3D is the best three-dimensional in 3D theaters, but has limited viewing angles; RealD 3D technology has the highest market share and does not Affected by the type of panel, any TV that supports 3D functions can restore 3D images. The disadvantage of polarized 3D technology is that two video output devices are needed to correspond to the left and right eyes, respectively. In a movie theater, it can be solved with two

projectors in parallel without loss of brightness and resolution. In home TV, the line resolution will be reduced by half with interlaced polarization.

Active shutter 3D mainly achieves the 3D effect by improving the refresh rate of the picture. By dividing the image into two frames according to the frame, two groups of pictures corresponding to the left and right eyes are formed, which are continuously interlaced and displayed. At the same time, the infrared signal transmitter The left and right lens switches of the shutter 3D glasses will be controlled synchronously so that the left and right eyes can see the corresponding picture at the correct time. This technology can maintain the original resolution of the screen, and it is easy for users to enjoy the true full HD 3D effect without reducing the brightness of the screen.

1.2.1.2 Naked-eye 3D technology

The naked-eye 3D technology is mostly in the research and development stage. Its research and development are divided into two directions, one is the research and development of hardware equipment, and the other is the display content processing. The second type has already begun small-scale commercial applications. From a technical point of view, naked-eye 3D can be divided into three types: light barrier technology [15], lenticular lens technology [16] and directional light source technology [17]. The biggest advantage of naked-eye 3D technology is to get rid of the shackles of glasses, but there are still many problems in resolution, viewing angle and viewing distance.

The principle of the light barrier technology is that after a slit grating is added in front of the screen, when the image that should be seen by the left eye is displayed on the LCD screen, the opaque stripes will block the right eye; similarly, the image that

should be seen by the right eye when displayed on the LCD screen, the opaque stripes will block the left eye. By separating the visible images of the left and right eyes, the viewer sees the 3D image.

The principle of the lenticular lens technology is to project the pixel points corresponding to the left and right eyes into the left and right eyes through the principle of refraction of the lens to achieve image separation. Compared with light barrier technology, the biggest advantage of this technology is that the lens will not block the light, so the brightness has been greatly improved.

The principle of directional light source 3D technology is to match two sets of LEDs, with a fast-response LCD panel and driving method, so that the 3D content can enter the viewer's left and right eyes in a sorted way to exchange images to generate parallax, so that people can feel the 3D effect. Its advantages are good resolution and light transmittance, and excellent 3D display effect.

1.2.2 3D technology in the future

In the previous chapter, I have introduced the current status of the development and use of 3D technology. These technologies make our life more and more convenient, and also allow us to see a more and more beautiful virtual world. Although these 3D technologies can show us a vivid world. However, if people watch the scenes generated by these 3D technologies for a long time, it will cause some discomfort more or less. For example, nausea, dizziness, cold sweats, etc. The reason for the appearance of these symptoms is roughly that the optic nerve feels a large-scale and high-frequency movement that does not match the physiological characteristics of the human eye. Therefore, it is not an

easy task to show a beautiful scene that matches the physiological characteristics of the human eye. However, holographic technology, as the ultimate form of 3D technology in the future, can solve all the problems of the current 3D technology. And it can meet all the physiological needs of human eyes to observe the three-dimensional scene (such as binocular parallax, motion parallax, accommodation and convergence) [18].

Holographic technology is a technology that uses the principles of interference and diffraction of light to record objects, and to truly redisplay the recorded objects. The term ”hologram” in holographic technology means ”all information of light”, and refers to the use of light projection to record and reconstruct all information (phase, amplitude, etc.) of light emitted by a recorded object. Holographic technology is also a kind of virtual imaging technology. Its imaging principle is to completely record the phase and amplitude of the object light wave emitted by the object by means of interference and diffraction of coherent light waves. At the same time, with the principle of light interference and diffraction to reproduce the recorded light wave information of the object, so as to achieve a realistic imaging effect.

Holographic technology is generally divided into two parts to reconstruct virtual objects. These two steps are generally called recording and reconstruction. The first step is to use the principle of light interference to record the information of the object light waves generated by the object, that is, the process of holographic shooting. When the recorded object is irradiated by a laser, part of the laser will form diffused reflection object beam, the other part of the laser beam hits the holographic plane as a reference beam, and interferes with the object beam to convert the phase and amplitude of each point on the object light wave into a spatially varying intensity, so that using the con-

trast and spacing between the interference patterns, all information of light waves can be recorded from this. The negative film, which records the interference patterns of the object's light wave information, becomes a hologram plane after a series of processing procedures such as development and fixing. The second step is to use the principle of diffraction of light waves to reconstruct the recorded light wave information of the object, which is the imaging process of holographic technology. The hologram recorded in the first step is like a very complicated grating. Under the irradiation of natural light or coherent laser, the diffracted light wave of a linearly recorded hologram can generally reproduce two images, namely the original image and the conjugate image. The reconstructed image looks very stereoscopic and has a true visual effect. This is because each part of the hologram completely records all the light information of each point on the object, so in principle, every part of it can be reconstructed, and the entire details of the original can be recorded on the same negative film through multiple exposures, and they can be clearly displayed separately without interfering with each other.

Computer-generated holography (which is short for CGH) is a novel technology that simulates the first step of traditional optical holography by a computer, that is, the step of recording light wave information of an object, and recording this light wave information as a digital data. Traditional holograms are formed by recording interference fringes generated by the interference of object light and reference light. Computer-generated holograms do not require two beams of light to be physically coherent. Compared with traditional optical holograms, the generation process of CGH is greatly simplified, so that CGH has been widely researched and applied. And since the German scientist Roman in the late 1960s proposed computer-generated holograms, this technology has

become an important branch of information optics. CGH technology has many advantages, for example, it can produce holographic animations, holographic games by generating continuous holographic images. However, CGH also has many disadvantages, one of them is the long calculation time caused by the huge amount of calculation.

1.3 The background of this thesis

We already know that the advantage of CGH over traditional optical holography is that it does not require a complicated optical system to record the physical interference process of two beams of light and can be able to generate animation or games, etc. But CGH technology, which is the ultimate goal of 3D imaging technology, still has many disadvantages, and one of them is the huge amount of calculation. Therefore, this thesis will foucus on the disadvantages of CGH's large amount of calculation and long calculation time, and propose some solutions to reduce the amount of CGH calculation and calculation time.

From games to professional training, such as virtual reality or mixed reality provide a novel way to immerse yourself in the experience. However, the current VR or MR technology has a fundamental challenge: presenting images with the extremely high resolution required for presence. This puts huge demands on the rendering engine and the transmission process. Head-mounted display devices often do not have sufficient display resolution, which limits the field of view and makes the experience worse. In order to drive higher resolution head-mounted display devices, traditional pipelines require high-end processing power, but even current high-end processors cannot achieve this. Although challenges will undoubtedly continue to emerge, research on improving

display resolution is also bringing us hope. In order to further improve the visual quality of 3D scene, the researchers proposed a method that takes advantage of human visual perception, which can achieve excellent visual quality with low computation and low power consumption, and can not affect the viewer's viewing experience at all.

1.4 The purpose of this thesis

Humans can usually see a field of view of about 160 degrees in the horizontal direction and 135 degrees in the vertical direction, but only within the range of 5 degrees in the center of the field of view can humans see the details of objects. This small area is called the fovea [19]. And after the resolution limit of the human eye exceeds this small area, it will rapidly decrease as the angular distance increases. In the field of VR, this characteristics of the human eye is used to reduce the resolution of fields other than the central field, thereby realizing an increase in the calculation speed of the head-mounted display device, which is called the foveated rendering technology [20]. In this thesis, my first proposed method is to use the foveated rendering technology to achieve a reduction in the amount of CGH calculations, thereby speeding up the calculation of CGH.

As you read this thesis, look around the room or look out through the windows of a moving train, your eyes are constantly in motion. However, the eyes do not see the scenery smoothly from one end to the other, but move from one point in the scene to the next quickly. This quick eye movement is called saccade. The visual system is usually very sensitive to movement, but humans are usually unaware of saccades. A saccade is the gaze-type eye movement with the largest amplitude and the fastest speed of human eye. It is an involuntary eye movement that occurs when the human eye tries to gaze.

In recent years, in the field of visual physiology, the interaction between saccade, visual perception and visual cognition has become a hot research topic.

Saccade is the fastest eye movement of the human eye (the fastest movement speed can reach 1000 degrees per second). Saccades occur in the unconscious state of humans at about 2 to 8 times per second, but saccades can also be generated by external stimuli. Due to external stimuli, saccades usually require approximately 200 milliseconds to respond to and occur from external stimuli. And depending on the magnitude of the eye movement, each saccade will last approximately 20 to 200 milliseconds [21]. After the saccade occurs, the human eye will suppress the visual signals transmitted from the retina to the brain for a period of time. That is to say, after each saccade, our brain hardly feels any visual information from the outside world. This phenomenon is called saccade suppression. The duration of visual suppression has an almost strict linear relationship with the movement amplitude of the saccade, so it can be thought that the greater the saccade amplitude, the longer the duration of the saccade suppression, so that after the saccade we can not feel the visual information from the outside will take longer. Based on this characteristic of the human eye, in CGH, we can use the feature that the human eye cannot obtain external visual information, and use eye tracking instruments to detect whether a saccade has occurred in the human eye. And after the saccade occurs, we can greatly reduce the resolution of CGH, so that the calculation amount of CGH and the calculation time of CGH can be greatly reduced. In this thesis, my second proposed method is to use the saccade suppression to achieve a reduction in the amount of CGH calculations, so that the calculation speed of CGH can be greatly promoted.

1.5 The structure of this thesis

This paper will consist of 8 chapters. In the first chapter, I introduced the current status and future of 3D technology development, and introduced my research background and purpose. In the second chapter, I will introduce the holographic technology and CGH rendering method in detail. In Chapter 3, I will introduce the FTOS device used in this thesis in detail. In the fourth chapter, I will introduce the foveated rendering technology in detail. In Chapter 5, I will introduce the first proposed method of this thesis in detail, the CGH high-speed calculation method using foveated rendering technology and the experiments and results. In Chapter 6, I will introduce the contents of saccade and saccade suppression in detail. In Chapter 7, I will introduce the second proposed method of this thesis in detail, the CGH high-speed calculation method using the saccade suppression and the experiments and results. In Chapter 8, I will summarize the content of this thesis and discuss the future prospects.

2

Holography

Holography refers to a technology that allows diffracted light emitted from an object to be reproduced in exactly the same position and size as before. Observing this object from different positions, the displayed image will also change. Therefore, the photos taken by this technique are three-dimensional (3D). The technique of holography can be used for optical storage, reproduction, and information processing. Although holo-

graphic technology has been widely used to display static three-dimensional pictures, the use of three-dimensional volume holography still cannot display objects arbitrarily.

In 1947, the Hungarian physicist Gabor (1900-1979) of the Hungarian descent from the Imperial College of Science and Technology in London discovered the holographic technology, and thus won the 1971 Nobel Prize in Physics. In 1956, Dennis Gabor invented holography or holographic photography.

Other physicists have also done a lot of groundbreaking work, such as Mieczyslaw Wolfke solved the previous technical problems to make optimization possible. This discovery is actually a product of a British company inadvertently improving the electron microscope. This technology was originally used by the electron microscope, so it was originally called ”electron hologram”. The hologram as an optical field did not start until the laser technology was invented in 1960. The first hologram recording a three-dimensional object was taken in the United States in 1962 by Yuri Denisyuk, Emmett Leith, and Juris Upatnieks. There are many kinds of holograms, such as projection hologram, reflection hologram, etc.

Holographic technology has many benefits, such as:

- The reconstructed three-dimensional image is conducive to the preservation of precious art materials for collection.
- Every point is recorded on any point of the hologram at the time of shooting. Once the photo is damaged, it does not matter.
- The holograms have a strong three-dimensional scene and vivid images, and can be displayed at various exhibitions with the help of lasers, which will get very

good results.

In this chapter, I will give you a detailed introduction to the recording and reconstruction process of holographic technology, as well as the details of computer-generated holographic technology.

2.1 The concept of holography

Ordinary photography can only record the intensity of the object's light field, it can not represent all the information of the object. Using the holographic method also records the intensity of the light field, but it is the intensity after the reference light interferes with the object light. For the light intensity recorded by this method, when the reference light is used for reproduction, the complex amplitude of the object light which comprehensively characterizes the object information can be expressed.

In order to take a satisfactory hologram, the shooting system must have the following requirements: According to the previous analysis, holography is based on the principle of light interference, so the light source must have good coherence. The emergence of laser provides an ideal light source for holography. This is because the laser has good spatial coherence and temporal coherence, and it can obtain a good hologram by shooting small diffuse objects. Because the interference fringes are recorded on the holographic negative film, and the interference fringes are thin and dense, the minimal interference in the photographing process will cause the interference fringes to blur, even making the interference fringes impossible to record. For example, if the film is shifted by one micrometer during the shooting process, the stripes cannot be clearly distinguished. For this reason, the holographic test bench is required to be shockproof.

All optical devices on the holographic table are firmly attracted to the steel plate of the worktop with magnetic materials. In addition, the airflow through the light path, sound wave interference and temperature changes will cause changes in the surrounding air density. Therefore, loud noises should not be allowed during exposure, and you should not move around at will to ensure that the entire laboratory is absolutely quiet.

The optical path difference between the object light and the reference light should be as small as possible. It is best that the optical paths of the two beams are equal, and the angle between the two beams should be around 45 degrees. The requirements are lower, and the intensity ratio of the two beams is appropriate. Because the thin and dense interference fringes are recorded on the holographic film, high-resolution photosensitive materials are needed. The rinsing process is also critical. We dispensed the drugs according to the formula requirements, and dispensed developer, stop fluid, fixer and bleach. All of the above prescriptions are required to be prepared with distilled water. The rinsing process should be carried out in a dark room. The liquid should not be exposed to light. The temperature should be maintained at about 20 ° C for rinsing. The prepared liquid can be used for about one month after proper storage.

In the next, I am going to introduce the processing of recording and reconstruction.

2.1.1 The recording part of holography

3D holographic projection technology is a technology to reconstruct the three-dimensional image of an object by recording the amplitude and phase distribution of light waves on a photographic film or dry plate. The holographic technology records all information (amplitude and phase) in the light waves reflected (or transmitted) by the object to re-

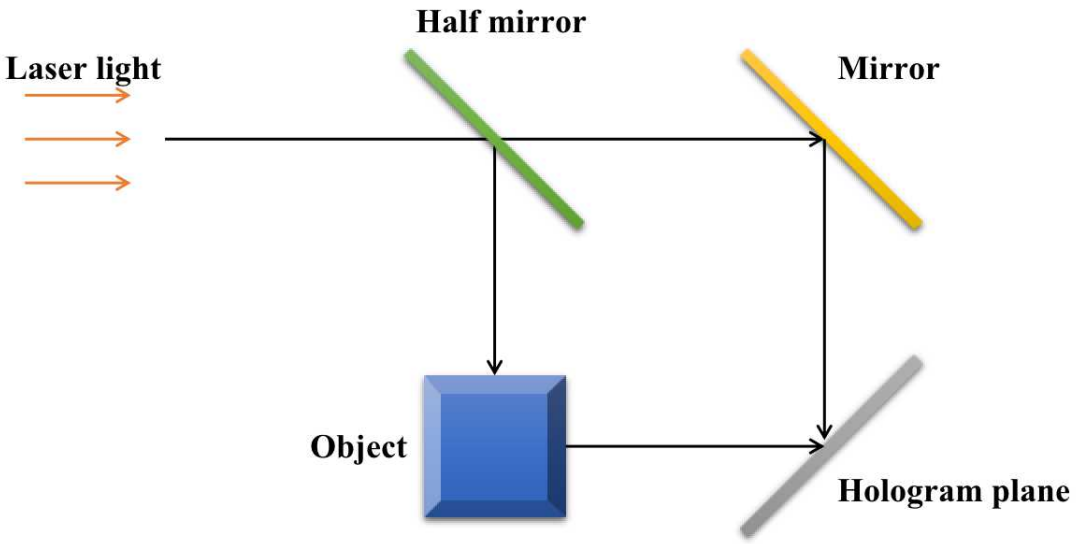


Fig. 2.1 The recording part of holography

alize 3D visual effects. The process is divided into two steps, one is recording and the other is reconstruction.

As shown in the Fig. (2.1).The first step is to use the principle of light interference to record the light wave information of the object, which is similar to the shooting stage of ordinary photography technology. Under the irradiation of pure laser, a part of the recorded object forms a diffusely reflected object light wave, and the other part reflects through the mirror as a reference beam to illuminate the holographic film, and the object light wave superimposes and interferes with each other. The amplitude and phase of the light source are converted into spatially varying light wave intensities, so that all the information in the object space is recorded using the spacing and contrast between the interference fringes. After processing the negative film with interference fringes through processing such as developing and fixing, it becomes a Nolid hologram, or a hologram for short.

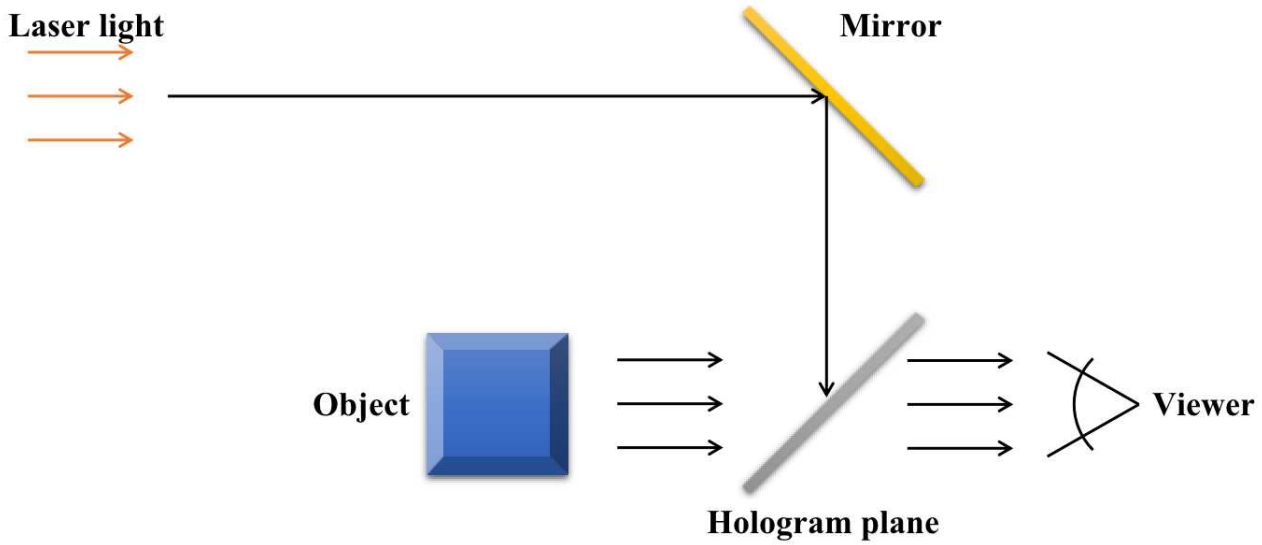


Fig. 2.2 The reconstruction part of holography

2.1.2 The reconstruction part of holography

After the process of recording in the previous chapter, a complete hologram can be successfully produced. As shown in Fig. (2.2). After generating a complete hologram, it is the process of reproducing the second part of the object. The principle is to use the principle of diffraction to reproduce the light wave information of the object recorded in the hologram. The hologram formed in the first step is like a complex grating in appearance. Under the irradiation of natural light or coherent laser light, the diffracted light wave of a linearly recorded sinusoidal hologram can generally give two images, namely the original image and the conjugate images. After the observer sees the reconstructed holographic image, it will form a very real visual effect. This is the process of 3D holographic reconstruction.

2.2 The Computer-generated Hologram

We already know the principle of traditional optical holography and its detailed manufacturing process. In this section, I will introduce the latest development branch of holographic technology, the computer-generated holographic technology.

The computer-generated hologram can record all the information of the object light waves of real or virtual objects, and the reconstruction image has the effect of physical depth of field and can be viewed with the naked eye, so it has great flexibility and unique advantages. In the historical process of optical development, after the introduction of computers into the field of optical processing, many optical phenomena can be simulated by computers, and only the holographic display is the reconstruction of the light wave amplitude and phase information of the original object, just like watching a real object or the same scene can provide all the three-dimensional information needed by the human eye. Therefore, this technology is considered to be the ultimate ideal three-dimensional display method.

2.2.1 Various advantages and disadvantages of CGH

CGH technology is the most potential naked-eye true three-dimensional display technology that has been developed in recent years by combining holography, optoelectronic technology and computer high-speed calculation technology. Comparing with traditional optical holography, CGH avoids the limitation of the actual recording optical path of the hologram, and can perform hologram calculation on the 3D data obtained by other means or the artificially made 3D model. It has the characteristics of flexibility and good repeatability.

Three-dimensional display is a visual process of recording, processing and reproducing the inherent three-dimensional information of an object. Integrated imaging method, stereo method, voxel method and holographic display technology are currently the main ways to achieve three-dimensional display. The integrated imaging method is displayed by combining a lens array and parallax images. The main disadvantage of this method is that the imaging focal length is fixed and the viewing angle is small. The stereoscopic rule is to obtain a 3D visual effect by wearing a device to watch the display. Such as 3D movies, HMD (helmet stereo display). The voxel method uses a high refresh rate projection device to project the three-dimensional information divided into multiple sections on the matching screen. However, the integrated imaging method, stereo method, and voxel method all use the parallax sense and visual persistence effect that naturally exist in the human eye to achieve the 3D effect. Essentially, the above three are not true three-dimensional display. Only CGH and optical holography can produce images with depth information, but compared with optical holography, the CGH has the following advantages:

- Optical holograms have high requirements on the sensitivity of recording media, and the complicated manufacturing process adds various factors that affect the imaging effect. CGH technology can simulate the optical holography process mathematically without introducing aberrations and noise.

- Optical holography has strict requirements for the light source used, and the experimental conditions for forming the light beam are the key to affecting the entire process. This limitation is eliminated in the computational holography method, and recording and reconstruction of holograms under various light source condi-

tions are realized.

- The complex amplitude distribution of the object field can be calculated and analyzed and compared, which greatly improves the accuracy and flexibility.
- CGH can be directly digitally stored, transmitted or reproduced analogly.
- Things that exist or don't exist in real life can be made and displayed through CGH, which expands the scope of application.

Based on the above points, we summarize the general flow of traditional optical holography and computer-generated holography, and show their detailed comparison in Fig. (2.3). Through Fig. (2.3), we can know in detail that CGH contrasts with traditional optical holography, which is convenient and quick in various steps, and can produce a variety of holograms.

In the next, I will introduce the various calculation methods for CGH in detail.

2.2.2 Various calculation methods for CGH

With the development of CGH, many types of methods for CGH have appeared, and their principles are similar and different, and they are used in different occasions. The first type is similar to ordinary optical holography. It can be divided into holographic stereogram method [22,23] which is a method to approximate continuous optical images in discrete form, Fourier transform method [24] which is the fourier transform of the object light wave by the computer with the help of fast fourier transform, wavefront recording plane method [25] which is a method that can reduce the amount of calculation by placing a special plane near an object, Look-up table method [26] which is a method

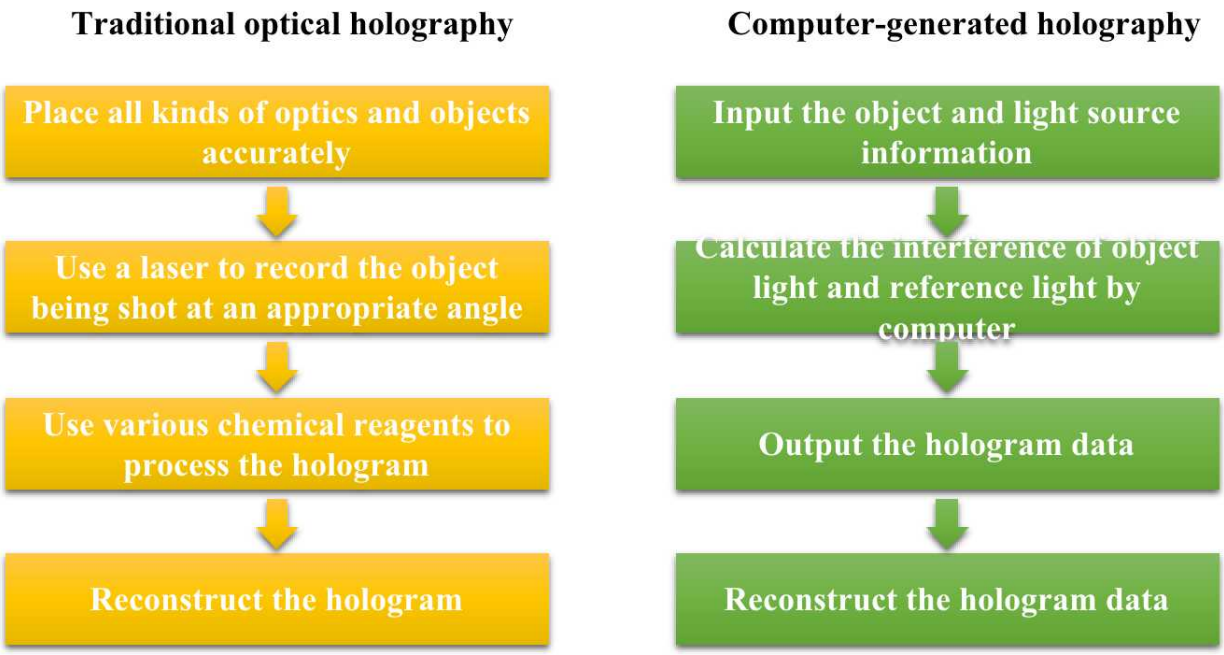


Fig. 2.3 The compare of traditional optical holography and CGH

that can preliminarily calculate a look-up table, and then achieve a significant reduction in the amount of heavy calculations in CGH, and the point-based method [27], which is used in my proposed method.

The second type is classified according to the nature of the hologram transmittance function distribution, which is divided into two types: amplitude type and phase type. In these two categories, according to the characteristics of the transmittance change, it can be subdivided into binary calculation holography and gray-scale calculation holography. Amplitude gray scale calculation hologram. Amplitude transmittance with only two values of 0 and 1 is an amplitude-type calculation hologram, which can be drawn by a common plotter, and is widely used because of its good anti-interference ability. The phase type calculation hologram does not attenuate the energy of light, the diffraction

efficiency is very high, and the quality of the hologram is high, but the manufacturing process is more complicated.

The third type is distinguished according to the coding technology used in the production of computational holograms, and is roughly divided into a circuitous phase type CGH and a modified off-axis reference light CGH. The detour phase hologram, which encodes the amplitude of light waves by controlling the transmittance or opening area of small cells on the hologram. The position of the rectangular hole is used to encode the phase of the object light wave. The entire recording process does not need to refer to the light wave or add an offset component. The modified off-axis reference light hologram simulates the optical conversion of the optical off-axis hologram on the computer, and realizes the superposition of the virtual off-axis reference light and the complex amplitude distribution of the light wave through transformation and calculation. The coding only needs to use the gray scale change or the aperture area at each sampling point of the hologram to make the complex amplitude distribution on the hologram plane into an intensity distribution, eliminating the need for phase coding.

In this thesis, the CGH calculation methods we used are all based on the point-based method to calculate the object light. In the following content, I will introduce the CGH calculation method we used in detail.

2.2.3 The point-based method

I have introduced several major categories of CGH calculations in the previous section. Among the many calculations of CGH, the calculation of object light is a particularly important part of CGH. In this thesis, the calculation of object light is based on the

point-based method of the first category in the CGH calculation category in the previous section. Then, the generation of the CGH interference pattern is generated using the ray-tracing method. Therefore, this section will introduce the detail of the CGH calculation method used in this study, namely the point-based method.

The point-based method is a very important method in CGH calculation. Generally speaking, this method is to cover the surface of each displayed object with many point light sources, and then use these point light sources to calculate the object light of the object. The advantage of this method is that even if the shape of the object is very complex and changeable, as long as enough point light sources are used to cover the surface of the object, it can show various details of the object very accurately and clearly. However, conversely, this method also has a very significant disadvantage, that is, as the shape of the object becomes more and more complex and more and more variable, we need to use more point light sources to cover the surface of the object to make sure that all objects are accurate and clear. As the number of point light sources continues to increase, the burden on the computer will also increase, which will also cause the amount of object light calculation to increase exponentially and the calculation time to increase exponentially.

First, I showed the detailed calculation of the point-based method in Fig. (2.4). As shown in the Fig. (2.4), I first assume that there is an object in the scene, and the surface of the object is covered with many point light sources, and the coordinate information of the point light source is represented by P_s. Therefore, the light wave information H of the point light source presented on the hologram plane can be calculated by the

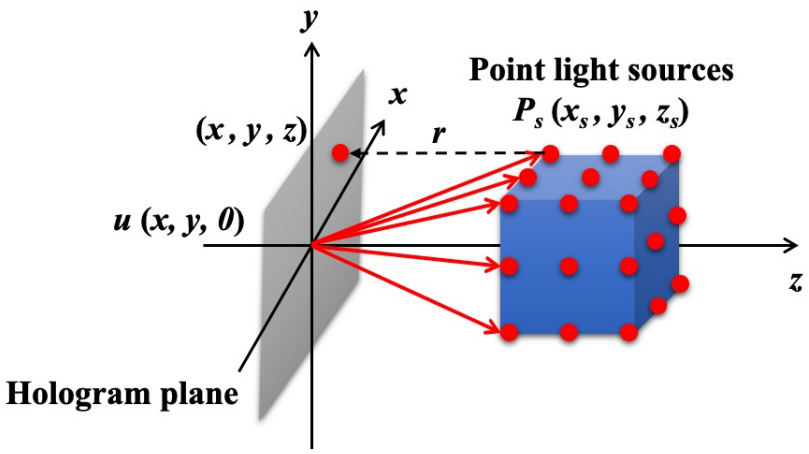


Fig. 2.4 The point-based method

following equation which is defined as

$$H(x, y, z = 0) = \frac{a}{r} exp(-jkr). \tag{2.1}$$

Where k is a constant (representing the wave number), its value is $2\pi/\lambda$, and a is the amplitude of the light wave information. r represents the distance between the point light source and the hologram plane, and r can be calculated by the following equation which is defined as

$$r = \sqrt{(x - x_s)^2 + (y - y_s)^2 + (z - z_s)^2}. \tag{2.2}$$

Based on the above equation, we can calculate the amplitude distribution of the point light source on the hologram plane. Therefore, when the number of point light sources becomes N, we can calculate all amplitude distributions of all point light sources on the

entire object on the hologram plane which is defined as

$$u(x, y, 0) = \sum_{s=1}^{N} (H(x, y, z = 0)). \tag{2.3}$$

Based on all the above equations, we can completely calculate the amplitude distribution of an object on the hologram plane. And, from the above equation, we can see that the calculation time of the point-based method is indeed multiplied by the number of follower point light sources.

2.2.4 The ray-tracing method

In the previous section, I have introduced the calculation method of CGH's object light in detail, namely the point-based method. In this section, I will introduce the calculation method used to generate the CGH interference pattern, the ray-tracing method.

Ray tracing is a method in which a ray tracing program mathematically determines and copies the route of light from an image, but in the opposite direction (from the eye back to the origin) [28, 29], as shown in Fig. (2.5). Ray tracing is now widely used in computer games and animation, TV and DVD production and movie products. Many manufacturers provide ray tracing programs for personal computers. In ray tracing, each ray path consists of multiple straight lines, almost always containing reflection, refraction, and shadow effects from the origin to the scene. In the animation, the position and direction of the straight part of each ray are constantly changing, so each ray must be represented by a mathematical equation, defining the spatial path of the ray as a function of time, according to the light before reaching the screen. One or more colors of the passing objects in the scene are assigned to each light. Every pixel on the

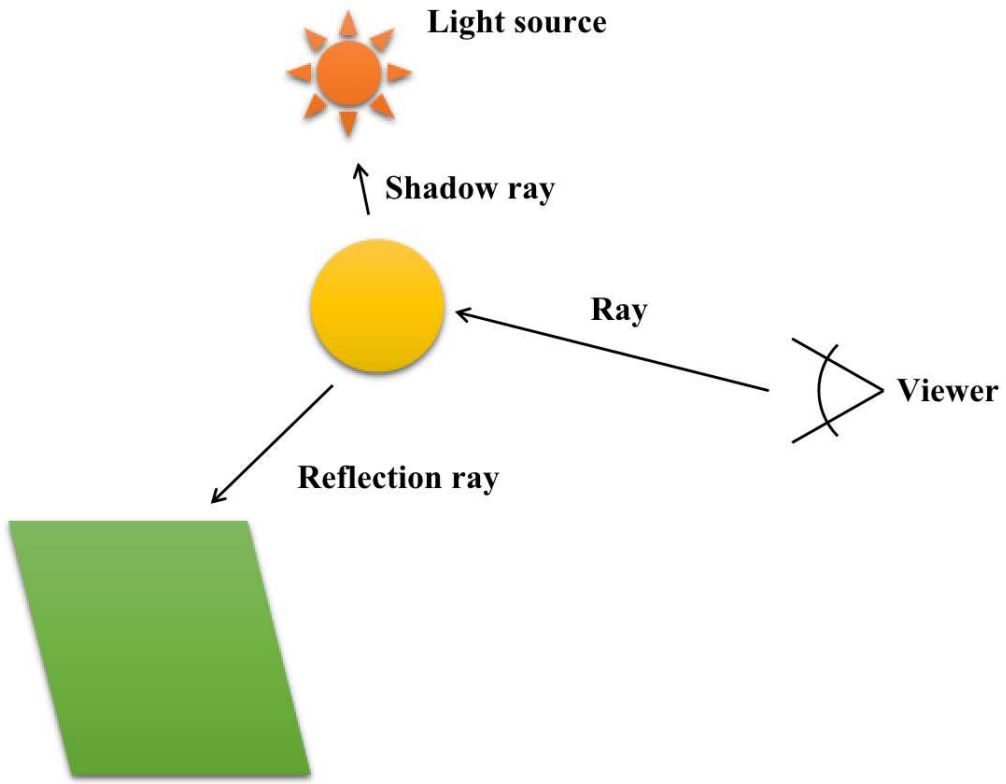


Fig. 2.5 The ray-tracing method

screen corresponds to every ray that can be traced back to the source at every moment. Ray tracing was first invented by scientists in an organization called the Mathematics Application Group in the 1960s [30]. Some of these scientists became interested in ray tracing as an art, becoming a painting artist, and established an animation photography studio to use ray tracing to produce 3D computer portraits and animations for TV and movies.

In my proposed method, the general calculation process of the ray-tracing method can also be represented in Fig. (2.4). First, we assume that the viewpoint is in the center of the hologram plane. Secondly, starting from the viewpoint, we project light

at a certain angle. Then, the projected light will detect whether it collides with the point light source covered by the object surface. If the light collides with the point light source on the surface of the object, then record the light source information of the point light source on the hologram plane. If there is no collision, the calculation will not be performed after the light reaches a certain depth (that is, the light will not be rendered, and no light source information will be recorded on the hologram plane). Finally, through the projection of many rays, we can record the light source information of all point light sources of all objects in the scene on the hologram plane. By applying the ray-tracing method to the field of CGH in this way [31], we can get a very real and beautiful CGH scene. And can also achieve functions such as reflection, refraction, perspective, shadow expression, highlight performance, hidden surface elimination and so on.

2.3 Digital holography

In the previous sections, I have introduced the calculation process of CGH in detail. Through these calculation methods, we can finally get the electronic data of the light wave information (recorded on the hologram plane) of all objects in the CGH scene, and these electronic data will be saved in the form of images. Therefore, when reconstructing these scenes recorded as electronic data, we need to use holographic reconstruction devices, which we collectively call digital holography. Digital holography is generally divided into two major categories, one is the ordinary digital holography device [32], and the other is the head-mounted digital holography device [33–35]. Regardless of the type of digital holography device, its components are roughly Spatial light modulator

(SLM), laser or LED light source, lens and mirror. Through these CGH regeneration devices, we can clearly see the CGH scene recorded in the hologram plane with the naked eye.

In this thesis, both method one and method two use ordinary digital holography device. Although the two are slightly different in parameters, the structure and principle of the two are the same, both are based on [32]. Regarding the detailed parameters and structure of the CGH device, I will introduce it in detail in the later experimental and results.

3

The fourier transform optical system

In the previous chapter, I introduced traditional optical holography, CGH and digital holography devices in detail. When using the digital holography device to reconstruct the CGH scene, there is usually a problem that the field of view is too small. Therefore, in this chapter, I will focus on introducing the fourier transform optical system (FTOS) [36] used in my method to solve the problem of the small field of view.

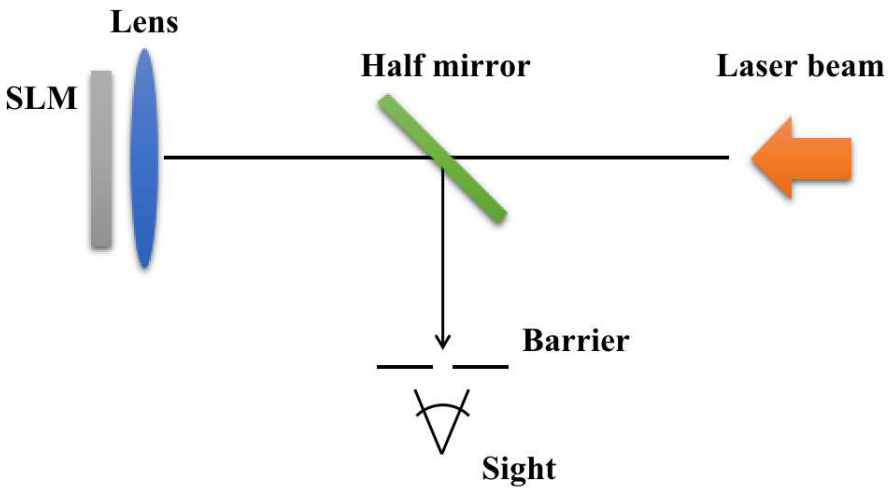


Fig. 3.1 The structure of FTOS

3.1 The concept and structure of FTOS

As I just mentioned, the purpose of FTOS is to solve the problem of too small field of view of traditional digital holography device. Compared with the traditional digital holography device, the structure of FTOS does not add too many optical components. Therefore, the principle and structure of FTOS can also be applied to these aspects for head-mounted CGH display devices that are mainly miniaturized and lightweight.

I show the structure of FTOS in detail in Fig. (3.1). It can be seen from the Fig. (3.1) that the main difference is that a convex lens is added in front of the SLM. It is this convex lens that can achieve the effect of expanding the field of view. Other structures, such as the role of the barrier, are to block the 0-th reflected light, and the position of the barrier must be set at a position of the focal length f of the convex lens from the half mirror. After such a structural setting, we can achieve the expansion of the field of view of CGH.

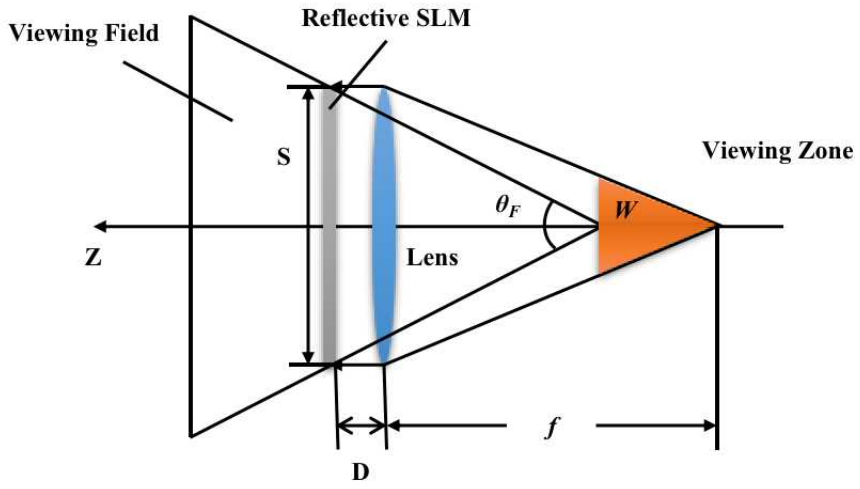


Fig. 3.2 The expansion of field of view by FTOS

The expansion of the field of view is explained in detail in Fig. (3.2). As shown in Fig. (3.2), the visible range of the SLM is enlarged through the convex lens, and finally the reconstructed image of the CGH can be observed within the scope of the viewing zone.

Also, regarding the expansion of the field of view, we can derive it based on the following equation which is defined as

$$\vartheta_F = 2 \cdot \tan^{-1}\left(\frac{S}{2(f+D)}\right). \tag{3.1}$$

In Eq. (3.1), the ϑ_F is the angle of the field of view, the S refers to the size of the SLM, f refers to the focal length of the convex lens used in FTOS, and D refers to the distance between the convex lens and the SLM (usually the convex lens is very close to the SLM, so in the approximate calculation, we can ignore this distance).

In addition, the W in Fig. (3.1) refers to the width of the visible range at the focal

point, and W can be calculated by the following equation which is defined as

$$W = \frac{\lambda f}{p}. \tag{3.2}$$

In Eq. (3.2), the p is the pixel pitch of the SLM, f is the focal length of the convex lens used in FTOS and the λ is the wavelength of the light.

Based on Eq. (3.1) and Eq. (3.2), we can conclude that FTOS can indeed expand the field of view of traditional digital holography devices, and FTOS is also very suitable for head-mounted CGH display devices.

3.2 Point light source position correction based on FTOS

In the previous section, I introduced the principle, structure, and corresponding calculation methods of FTOS in detail. But we know that for any optical system that uses a convex lens, due to the use of a convex lens, the final imaging will be more or less distorted, and the FTOS system is no exception. Therefore, in order to solve the problem of CGH reconstructing image distortion, we must correct the image distortion during calculation.

We show the schematic figure of FTOS point light source position correction in Fig. (3.3). From the Fig. (3.3), we can see that the point light source information Q recorded on the hologram plane, after the change of the convex lens, will be imaged on the point P without correction. Obviously, if this is the case, in the final CGH reconstruction image, the entire scene will have very obvious distortion. Therefore, we must correct the distorted point light source P to the correct position, the point O.

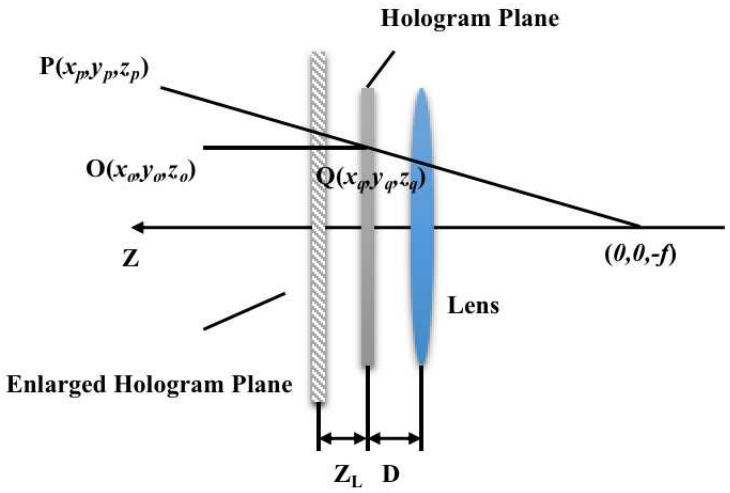


Fig. 3.3 The position correction for FTOS

The three coordinates of the point light source O can be calculated by the following equations which are defined as

$$x_O = x_P z_O B, \tag{3.3}$$

$$y_O = y_P z_O B, \tag{3.4}$$

$$z_O = -\frac{fA}{f - A}. \tag{3.5}$$

In these three equations, (x_P, y_P, z_P) is the three coordinates of the uncorrected point P, and (x_O, y_O, z_O) is the coordinate O of the correct point light source. Also, the A and B shown in these three equations can be calculated by the following euqations which are defined as

$$A = \frac{z_P(f - D) + D^2}{z_P - D - f}, \tag{3.6}$$

$$B = \frac{A + D - f}{Af}. \tag{3.7}$$

Based on all the above equations, we can correct the distortion caused by the convex lens, so that we can restore the correct CGH scene, ensuring that the observer will not have any abnormalities when watching the CGH scene.

4

Foveated rendering

4.1 The concept of foveated rendering

In traditional CG graphics rendering, it is usually independent of the gaze position of the human eye, and the entire screen will be rendered with extremely high resolution. In the past, when the resolution of the display itself was not too high, the screen rendering could be done in this way. But nowadays, as the resolution of monitors improves, 4K

and even 8K monitors have gradually entered our daily lives. In such a high resolution situation, the high resolution rendering of the entire screen will place an extremely serious burden on our CPU and GPU.

In our broad field of vision, only a small part of it is highly concentrated. Anything beyond the center of our gaze zone by more than 5 degrees will gradually reduce the resolution, due to the different concentration of cone cells on the retina responsible for observing color and detail. The area with high-density cone cells is called fovea, which corresponds to the point of gaze in our field of vision. When the human eye is looking at something, not the entire field of view is as clear, instead, the resolution in the middle of the screen you are looking at is the highest, and the resolution decreases in turn toward the surroundings. Therefore, when displaying an image on a monitor or a virtual reality device, rendering the entire screen with extremely high resolution is a serious waste of computing resources. It is not necessary that the entire screen has the same high resolution, but the resolution in the middle of the screen you are looking at is the highest, and the surrounding resolution can be lowered in order.

In traditional display devices, the area of the 5 degrees fovea region only accounts for about 7% of the display of 60 degrees, and for head-mounted devices with a wider field of view, the area of the fovea region will occupy a smaller percentage. In this case, when we display the 3D scene, we only need to track the user's eye movements, and perform high-resolution rendering of the user's gaze position, and low-resolution rendering of the remaining areas. We call this rendering technique foveated rendering technology. And, there have been many researches on this technology. Some papers elaborated on the application of eye tracking [37], eye tracking technology applied to

3D graphics [38], the application of multi-resolution gaze point display devices [39, 40] and some points of attention in the design of display devices [41]. There are also some papers that describe the effect of reducing the resolution of areas outside the fovea on visual search performance [42], and prove that the resolution of areas outside the fovea can be reduced by nearly half without significantly reducing the visual search performance [43], and examined that in the large field of view (20 degrees to 30 degrees of field of view) using the field blur effect outside the fovea region, the resolution control affects the visual search better than the size control of the field performance.

In my proposed method, I applied the foveated rendering technology to the CGH field, using the highest sampling interval (that is, the angle of rays) to render within 5 degrees of the center of the gaze point, and the surrounding areas are rendered in lower sampling interval.

4.2 Visual acuity

There is a small depression on the inside of the back of the human eye, called a ”fovea”. The small concave is the only place on the retina that can guarantee 100% clear imaging. This area occupies a very small area in the real field of view. In other words, although the human eye has a wide field of vision, it can really be perfectly resolved, and the area with 100% resolution is guaranteed to be only a pitiful piece; we also understand this in daily life, except for a small piece focused in front of our eyes, the afterglow on both sides is basically indistinct; on the retina, a place that does not receive enough resolution to image is called a “Optic disc” or “Blind spot”, as shown in Fig. (4.1) [44]. In real life, the reason why we can see more comprehensive and clear images is because

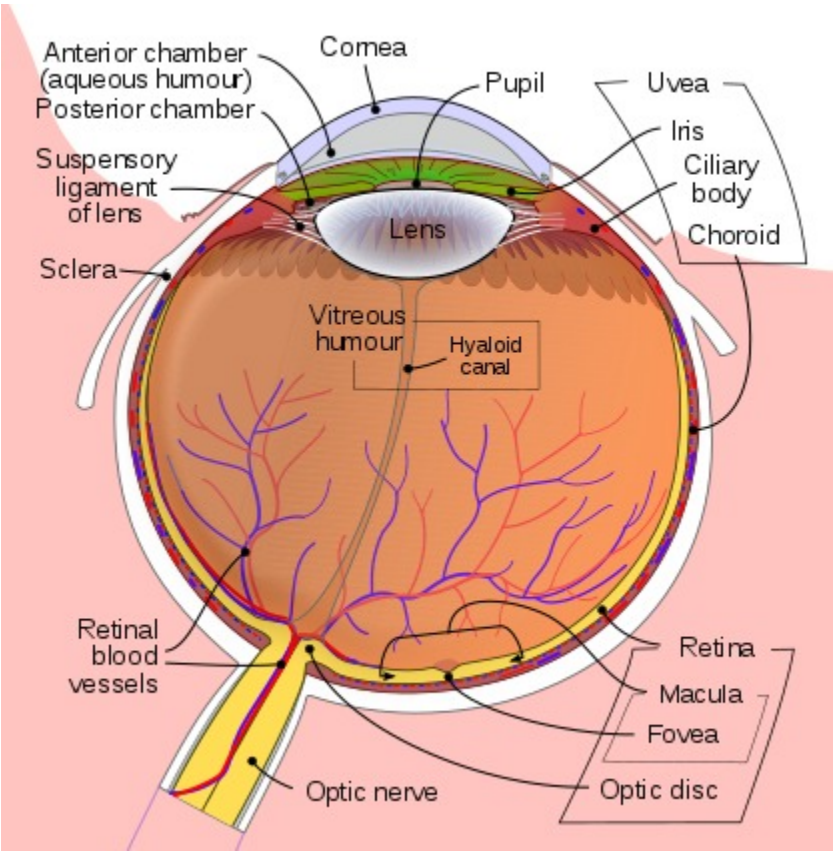


Fig. 4.1 Eye structure

our eyeballs are constantly moving (including subconscious movements). In this way, the eyes can collect high-resolution visual signals in the entire area, and then our brain synthesizes and processes them, and a beautiful world is displayed before our eyes. Therefore, the visual acuity of the human eye is incomparable with the resolution in optical.

Based on this characteristics of the human eye, many scientists have done the researches on how the resolution limit of the human eye outside the fovea region changes with the change in angular distance. H.Strasburger [45] made a very detailed summary

of how the resolution limit of the human eye in the surrounding area changes. We know from the research of Strasburger H that the resolution limit of the human eye with the angular distance can almost be said to be a very standard linear relationship. This linear relationship can be summarized by the following equation which is defined as

$$\alpha = me + \alpha_{\circ}, \tag{4.1}$$

where α means the resolution limit of human eye, e is the change in angular distance outside the fovea region, $\alpha_{\circ}$ is the smallest resolution limit of the human eye in the fovea region (that is, when $e = 0$, and we decided to take $\alpha_{\circ}$ as the minimum resolution limit in the case of normal human visual acuity of 1.0, 0.017 degrees), and m represents the slope, which is a constant number in this equation.

Based on this linear equation, we conclude that when the foveated rendering technology is actually applied, we can use this equation to calculate how much resolution we have to meet outside the central concave 5 degree range that human eye needed. This will greatly reduce the amount of CGH calculation and greatly increase the speed of CGH calculation.

4.3 Some conventional methods using foveated rendering

We already know that the resolution limit of the human eye varies linearly with angular distance. And in the field of CGH, there already have been some researches on the application of foveated rendering to CGH. One of them is about applying the foveated rendering method at the hardware level [46]. This method is mainly to combine the 2D

image with the CGH reconstruction image, and apply the foveated rendering method. The research is to place the 2D image after 1 meter from the hologram (and the 2D image represents the area outside the foveal region of foveated rendering), and place the hologram in the center of the entire scene, representing the fovea region. Therefore, in this method, not the entire scene is CGH; and the reduction of the resolution of the surrounding area is only a reduction of the pixels of the 2D image, not the reduction of the resolution of CGH. Moreover, since the surrounding area is 2D, the depth of field cannot be adjusted freely. Another method is to reduce the resolution of the surrounding area by reducing the number of rays in the surrounding area of the entire CGH scene [47]. But this method will cause gaps in the surrounding area, and will affect the observer to watch the CGH scene.

In my proposed method, we can freely control the size, position, depth, etc. of the CGH scene, and there will be no gaps, nor will affect the observer's viewing the CGH scene.

5

CGH high-speed calculation using foveated rendering

In the previous chapters, I have introduced various contents of computer-generated holography in detail. Therefore, in this chapter, I will begin to introduce my first proposed method, which is using foveated rendering for CGH.

As I said before, foveated rendering was originally proposed in the field of CG and was applied to head-mounted display devices. From this successful application, we can know that it is very feasible to improve the traditional CG rendering by using the characteristic that the human eye can only clearly see the objects in the central 5 degrees. Therefore, I decided to apply foveated rendering to the field of CGH to achieve the purpose of high-speed calculation of CGH.

5.1 Overview of the proposed method using foveated rendering

I have introduced the method of applying ray tracing to CGH, which can make the whole CGH scene more realistic and gorgeous. In the previous researches, we have also known many conclusions about the changes in the sensitivity of the human eye from the fovea region to the surrounding area. And based on the conclusions of these experiments, I will use representative results in my method. Therefore, in general, my method is mainly to render the CGH reconstructed image into two regions: the center region (which can be also called fovea region) that the human eye is looking at and the outer region outside the center region. In the center area (the area within 5 degrees of the gaze point), the reconstructed image of CGH will be rendered at the highest resolution of our device, while the resolution of the outer area will be rendered at half the resolution of the center area. Based on the parameters of our holographic device, after expanding the field of view through FTOS, we can display the reconstructed image of CGH within 8 degrees. Therefore, outside the 5 degree range of the center of the field of view, that is, between 5 degrees and 8 degrees, I will render the CGH image at half the resolution of the center area. However, in the experimental part, I still set the resolution of the

external area to several different levels (such as half, quarter, one-eighth, etc.) to prove whether the external resolution will influence the observer to watch the entire CGH reconstructed image.

5.2 CGH resolution based on Fresnel zone plate

We already know that when using foveated rendering, we do not need to render the peripheral area (area outside the 5 degree range) of the CGH reconstructed image at the highest resolution. Therefore, in order to reduce the amount of calculation, we need to reduce the resolution of the peripheral area. However, for CGH, we cannot reduce the resolution by reducing the number of pixels in the image like CG images. Therefore, we need to reduce the resolution of CGH through another method. When I introduced the calculation method of CGH, I mentioned that my method is to use ray tracing to render the CGH image, and the basic principle of ray tracing is to project countless rays to render the entire scene. Therefore, in order to reduce the resolution of the peripheral area of CGH, we can reduce the number of rays, which means expand the ray angle in the peripheral area to achieve this goal as shown in Fig. (5.1). However, it is not enough to simply increase the angle between the light rays, beacuse this will make a very clear gap between the point light source and the point light source when the CGH reconstructed image is actually observed, as shown in Fig. (5.2). As we can see in the Fig. (5.2), without any treatment, if the angle between the rays is enlarged, the original continuous plane will become a discrete point light source. In this case, when observing the CGH and reconstructing the image, it will have a great impact on the observer. Therefore, in order to solve this problem, we must find a way to fill the gap between these discrete

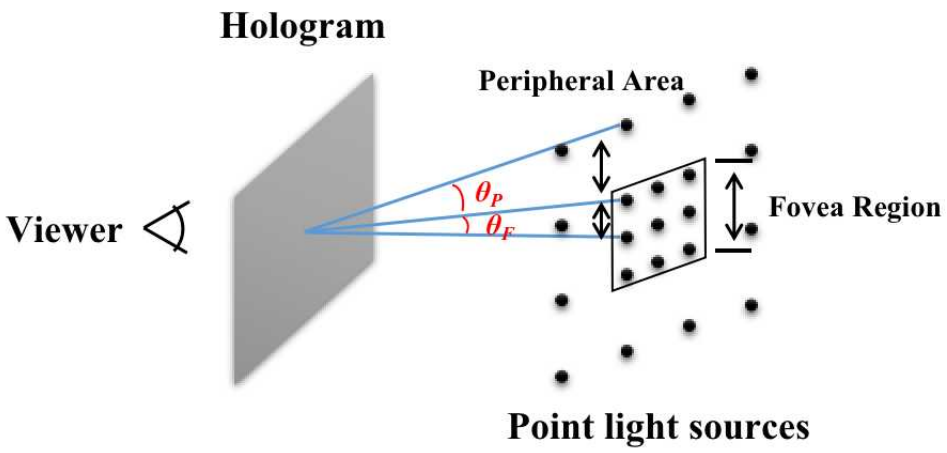
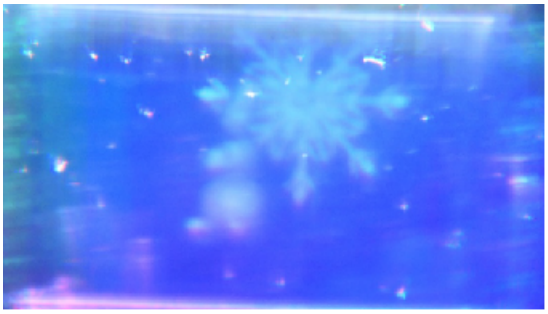


Fig. 5.1 Reduce the ray number by expanding the ray angle



Continuous surfaces of snowman



Discrete points of snowman

Fig. 5.2 Example of snowman

point light sources.

The zone plate is composed of alternating transparent and opaque rings to block the odd or even bands in the half Fresnel zone plate. Under the illumination of point light source, the diffraction characteristics of high-intensity point light of zone plate can be obtained through it. The production of the classic Fresnel zone plate can be done by manual drawing, and then it can be finished twice by the camera. It can be seen that the transformation effect of a wave plate on the wave front is equivalent to the function of

both a convergent lens and a divergent lens. The main components of its diffraction field include a series of converging spherical diffracted waves, a series of divergent spherical diffracted waves, and of course, a plane wave (or directly transmitted wave) component that travels straight along the incident direction. The zone plate has the advantages of large area, light weight, and foldability, and is particularly suitable for long-distance communication, optical ranging, and aerospace technology. And the focal length of the zone plate is shortened with the increase of the wavelength. The diffraction law is used to intentionally change the wave front to create the diffraction field that people need. The zone plate has an amplitude type and a phase type; a black and white type and sinusoidal wave type zone plate with transmission function only taking 0 and 1, and there are also sound wave and microwave type zone plate. The Fresnel zone plate belongs to the amplitude type black and white optical zone plate. The application of the zone plate is more and more extensive, and the design and preparation of various zone plate is developing into a specialized technology.

In CGH, after the point light sources on the surface of all objects are recorded, what appears on the hologram plane is a collection of many zone plates, as shown in Fig. (5.3). After these zone plates are reconstructed by the digital holography device, a complete CGH reconstruction image will be presented. Moreover, according to Rayleigh theory, the size of the point light source reconstructed by the zone plate is determined by the radius of the zone plate [48] which is defined as

$$\omega_{ZP} = C \cdot \lambda F. \tag{5.1}$$

In the Eq. (5.1), C is a constant number (usually its value is 1.22), λ is the wave-

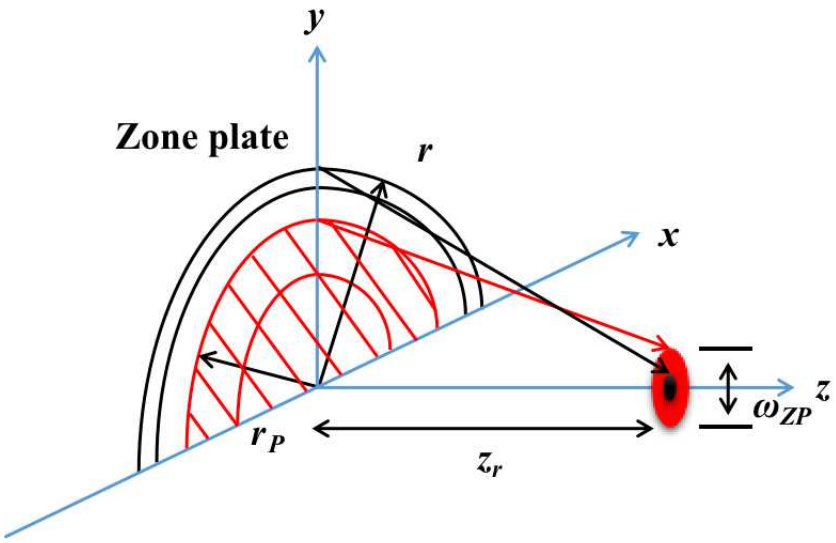


Fig. 5.3 The relationship between zone plate and resolution limit

length of the light wave, and F represents the ratio between the absolute value z_r representing the depth coordinate of the point light source and the zone plate diameter $2r$. Therefore, we can also rewrite the Eq. (5.1) into the following which is defined as

$$\omega_{ZP} = C \cdot \lambda \cdot \frac{|z_r|}{2r}. \tag{5.2}$$

Based on the Eq. (5.1) and Eq. (5.2), in order to fill the gap between the point light sources caused by the larger angle of ray, we can fill the gaps by increasing the size of the point light source. Moreover, increasing the size of the point light source can be achieved by reducing the radius of the zone plate. In summary, we can increase the point light source by reducing the radius of each zone plate in the peripheral area of the fovea region to fill these gaps.

5.3 The luminance of point light sources based on Fresnel zone plate

In the previous section, I have introduced the control of CGH resolution and the relationship between the point light source and zone plate in detail. This can make the point light source in the peripheral area of the fovea region larger and blurry, which can fill the gap caused by the larger angle of the ray, and will not affect the observer's viewing CGH reconstruction image due to the blur. However, also according to the theory of the zone plate, after reducing the radius of the zone plate, the intensity of the diffracted light will also decrease, and the luminance of the point light source will decrease greatly as the radius of the zone plate decreases. Therefore, in order to solve the luminance problem, we must properly correct the luminance of the point light source when rendering the CGH reconstruction image.

First of all, we know that for a camera, the amount of light entering is proportional to the aperture area of the lens [49]. Based on this phenomenon, for CGH, the luminance of the point light source is inversely proportional to the square of F (which is shown in Eq. (5.1)). Due to this, we can conclude that the luminance L_p of the point light source can be obtained by the following equation which is defined as

$$L_p = C_p \cdot \frac{1}{F^2}. \tag{5.3}$$

C_p in the Eq. (5.3) is a constant number. And since F in the Eq. (5.3) can be expressed by the absolute value of the depth of the point light source and the radius of the zone plate, we can rewrite the Eq. (5.3) into the following equation which is defined

as

$$L_R \propto r^2. \tag{5.4}$$

From Eq. (5.4), we can see that the final luminance of the point light source is proportional to the square of the radius of the zone plate. This means that when the radius of the zong plate is reduced to one-half, the luminance of the point light source will be reduced to one-quarter. Therefore, when we want to fill the gap caused by the larger angle of the ray, we reduce the radius of the zone plate to make the point light source larger and blurred. At the same time, the luminance of the point light source should be corrected by a multiple of the square of the percentage reduced by the radius of the zone plate. Therefore, before finally performing CGH rendering, we must increase the a in Eq. (2.1) according to the multiple of the need to correct the luminance of the point light source to solve the problem of luminance reduction caused by the reduction of the radius of the zone plate. In this way, we can ensure that the observer will not be affected by the luminance problem when viewing the CGH reconstruction image.

5.4 CGH fast calculation with foveated rendering

In the previous chapters, we already know that in the field of CG, the use of foveated rendering can greatly reduce the pressure on the computer of screen rendering, and can greatly speed up the calculation. Therefore, my method is to apply foveated rendering to CGH, in order to solve a long-standing problem of CGH, that is, the calculation speed is too slow due to excessive calculation. Through the introduction of this chapter, we can know that the reason for applying foveated rendering to CGH to speed up the calculation speed is mainly due to the following two reasons: 1. In order to reduce the resolution of

the peripheral area other than the fovea region, the amount of ray in the peripheral area is reduced, thereby reducing the calculation amount. 2. In order to fill the gap between the point light sources caused by the reduction in the amount of ray, thereby reducing the calculation amount caused by the reducing of the radius of the zone plate. Therefore, in order to prove that these two points can indeed reduce the calculation amount of CGH, we need to first rewrite Eq. (5.2) into the following equation which is defined as

$$r = \frac{\lambda \cdot C}{2\vartheta}. \tag{5.5}$$

Moreover, we know that for traditional CGH calculations, the computational complexity O can be expressed by the following equation which is defined as

$$O(\frac{L^4 r^2}{\vartheta^2}), \tag{5.6}$$

and by bringing Eq. (5.5) into Eq. (5.6), we can get the following equation which is defined as

$$O(\frac{L^4}{\vartheta^4}), \tag{5.7}$$

or we can get the equation which is defined as

$$O(L^4 r^4). \tag{5.8}$$

In these equations, L represents the size of the hologram plane, ϑ represents the angle of light, and r represents the radius of the zone plate. For my method, I mainly divide the entire CGH into two parts for calculation, one part is the same as the traditional

CGH calculation which is the fovea region, and the other part is the peripheral region with reduced resolution. Therefore, for the fovea region, the computational complexity can be expressed by the following equation which is defined as

$$O_F(\frac{\Phi^4}{\vartheta^4}), \tag{5.9}$$

or we can expressed by the following equation which is defined as

$$O_F(\Phi^4 r^4), \tag{5.10}$$

and for the peripheral area, we can use the following equation to express which is defined as

$$O_P(\frac{L^4 - \Phi^4}{\vartheta_P^4}), \tag{5.11}$$

or we can also express like

$$O_P((L^4 - \Phi^4) r_P^4). \tag{5.12}$$

In Eq. (5.9), Eq. (5.10), Eq. (5.11) and Eq. (5.12), Φ represents the size of the fovea region, and ϑ_P represents the angle of light in the peripheral area and the r_P is the radius of the zone plate outside the fovea region. From the four equations from Eq. (5.9) to Eq. (5.12), we can see that for foveated rendering, in order to reduce the amount of ray caused by the reduction of the resolution in the peripheral area, and to reduce the radius of the zone plate in the peripheral area to fill the gap between the point light sources caused by the reduced amount of ray, the reduction in calculation amount is as many as the fourth power of these two changes. Therefore, we can conclude that by applying

Table 5.1 Parameters of computer for CGH with foveated rendering

CPU	Intel Core(TM) i7-6700
OS	Windows 7 Professional 64 Bit
RAM	8.0 [GB]
Clock Frequency	3.40 [GHz]
GPU	NVIDIA GeForce GTX TITAN

the foveated rendering to CGH, it will reduce the amount of CGH calculations and thus increase the calculation speed greatly.

5.5 Experiments and results for CGH with foveated rendering

5.5.1 Experimental environment and devices for CGH with foveated rendering

First, I will introduce the experimental details of the first proposed method. This experiment included three theoretical verification experiments and a subjective experiment. The theoretical verification experiment mainly includes CGH resolution experiment, CGH luminance experiment, and CGH calculation time comparison experiment. The main content of the subjective experiment is to confirm whether the observer can feel the abnormality of the CGH reconstruction image and the observer 's evaluation for the CGH reconstruction image. The detailed parameters of the computer used in the experiment and the detailed parameters and appearance of the digital holography device are shown in Table. (5.1), Table. (5.2) and Fig. (5.4).

5.5.2 Experiment and results for CGH resolution

In this part of the experiment, the main purpose is to confirm the relationship between the resolution limit and the radius of the Fresnel zone plate. Based on Eq. (5.2), we can

Table 5.2 Parameters of holographic display for CGH with foveated rendering

Pixel pitch of SLM	9.6×9.6 [μm]
Number of pixel	1,280×768 [pixels]
Resolution limit	0.05°
Field of view	8°[H] x 5°[V]
Wavelength of each color	Red:625 [nm] Green:525 [nm] Blue:465 [nm]

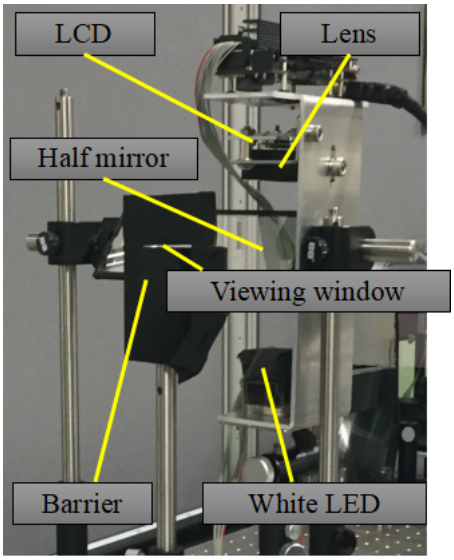


Fig. 5.4 Holographic display for CGH with foveated rendering

already know that, theoretically, when the radius of the Fresnel zone plate is smaller, the resolution limit of the CGH reconstructed image will be worse, that is, the point light source will become larger and more blurry, then, the overall resolution of the CGH reconstructed image will be lower.

Therefore, in order to prove the correctness of Eq. (5.2) by experiment, I first made a CGH reconstructed image, as shown in Fig. (5.5). In Fig. (5.5), we can see that there are many red rectangles in the middle of the figure, and there is a certain gap between each two rectangles. I strictly set the position of each rectangle to ensure that the gap size

between each two rectangles is 0.025 degrees, 0.05 degrees, 0.075 degrees, 0.1 degrees, 0.125 degrees, 0.15 degrees, 0.175 degrees and 0.2 degrees from right to left. From Table. (5.2), we can know that the resolution limit of our holographic device is 0.05 degrees. Therefore, in Fig. (5.5), the rightmost gap cannot be observed (because the angle of the gap is less than 0.05 degrees, our holographic device is indistinguishable).

Therefore, I predict that after I reduce the radius of the Fresnel zone plate, the point light source will become larger and larger and more and more blurred. And then, starting from the far right in the figure, gradually more gaps will be filled and become more and more blurred. The different results after reducing the Fresnel zone plate are shown in Fig. (5.6). From the results in Fig. (5.6), we can see that as the radius of the Fresnel zone plate becomes smaller and smaller, the gaps between the rectangles become more and more blurred and more and more indistinguishable. Until the end, the entire image could not distinguish any gaps and became very blurry. From this result, we can know that the resolution of the CGH reconstructed image is indeed determined by the radius of the Fresnel zone plate, and as the radius decreases, the overall resolution becomes worse. Also, we summarize the radius of the Fresnel zone plate and the resolution of the CGH reconstructed image into Fig. (5.7). This result is also fully consistent with the result of Eq. (5.2). Finally, we concluded that these results confirm the theoretical correctness of my proposed method.

5.5.3 Experiment and results for luminance

In the previous section, I have demonstrated the relationship between CGH resolution and Fresnel zone plate. Therefore, the effectiveness of my proposed method for reso-

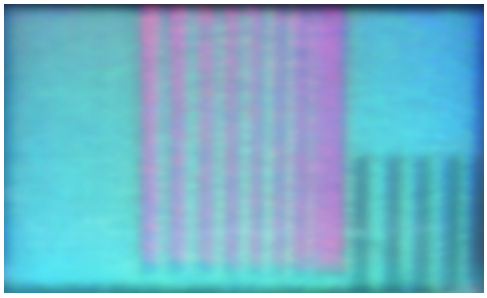
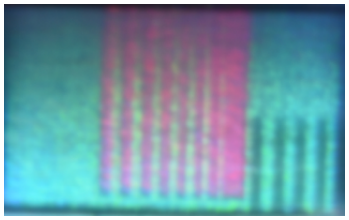
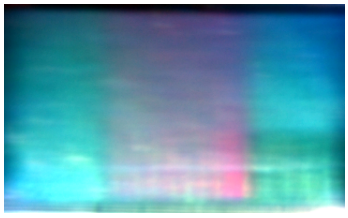


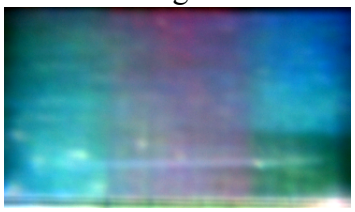
Fig. 5.5 CGH reconstruction image without changing the radius of zone plate



(a) 1/2 radius of the original Fresnel zone plate



(b) 1/4 radius of the original Fresnel zone plate



(c) 1/8 radius of the original Fresnel zone plate

Fig. 5.6 Reconstruction images with different radius of Fresnel zone plate

lution control of CGH reconstructed images is proved. In this section, I will introduce the correction method about luminance.

As shown in Eq. (5.4), we have concluded that the luminance of the CGH point light source is proportional to the square of the radius of the Fresnel zone plate. Therefore, when the radius of the Fesnel zone plate becomes one-half, the luminance of its point light source will become one-quarter. But we know that it is very difficult to directly detect the luminance change of the point light source, so we must use other methods to detect the luminance. For a camera, the amount of light entering the lens is proportional

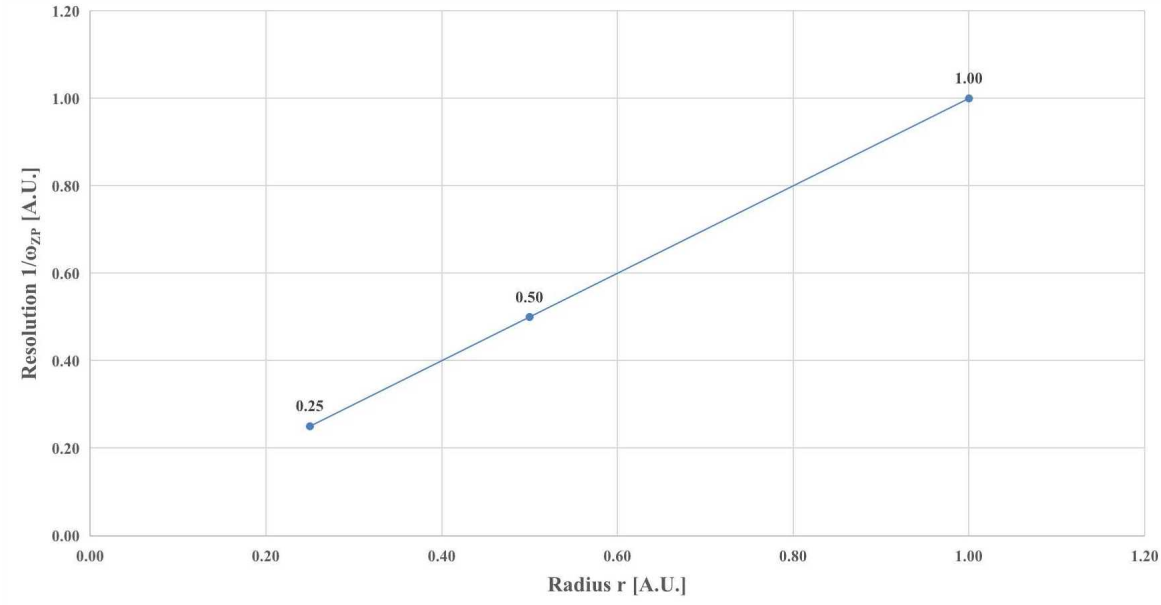


Fig. 5.7 Relationship between CGH resolution and radius of Fresnel zone plate

to the exposure time without changing any other parameters. For example, when the exposure time is doubled, the amount of light entering is also doubled. Therefore, we can control the other parameters of the camera to remain unchanged, and on the premise of only changing the exposure time, the relationship between the measured light amount and the RGB value after the actual imaging can be measured. After knowing the relationship between the amount of incoming light and the RGB value, we can use this measured functional relationship to detect the RGB value of the CGH interference pattern to know the multiple of the change in the luminance of the point light source.

After the measurement, the relationship between brightness and RGB value is obtained, I change the radius of the Fresnel zone plate to the original one-half, one-third, one-quarter, which means that in theory, the luminance of the point light source will become one-quarter, one-ninth and one-sixteenth. And then, I substituted the average

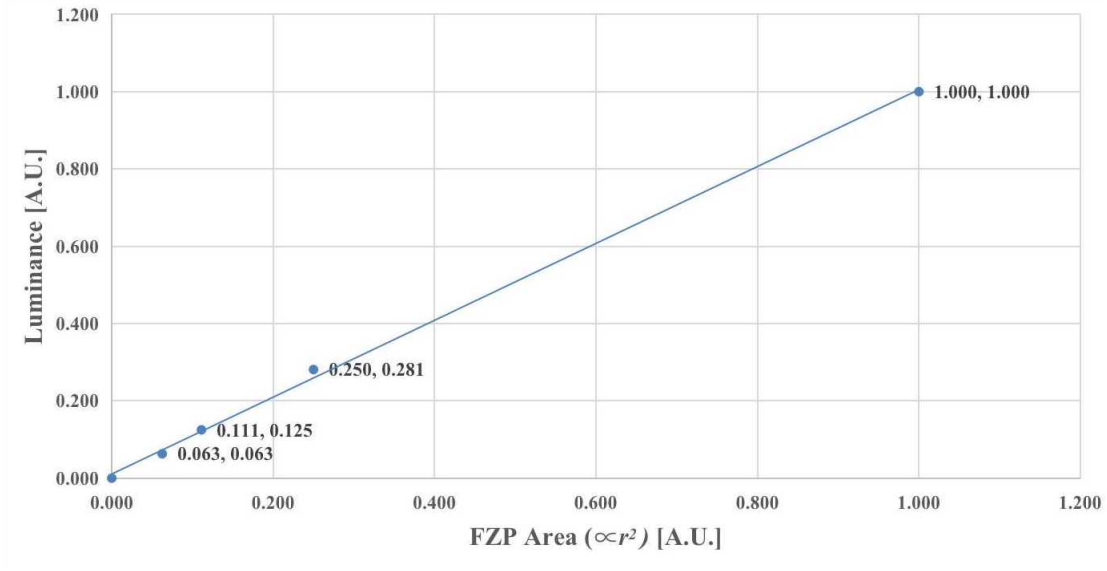


Fig. 5.8 Luminance changed with the area of Fresnel zone plate

value of the measured RGB values into the relationship between the luminance and RGB, and obtained the actual point light source luminance variation. The results are shown in Fig. (5.8). From the results in Fig. (5.8), we can know that the actual measured luminance change is almost consistent with our predicted theoretical luminance change, that is, the ratio of the luminance change to the square of the radius of the Fresnel zone plate is almost perfect linear relationship. This result also proves the correctness of our Eq. (5.4) and the feasibility of correcting the luminance changes.

Now that we have proved the correctness and feasibility of the luminance correction method. We can actually correct the luminance of the point light source to ensure the observability of the CGH reconstruction image, that is, to ensure the consistency of the overall luminance of the peripheral area and the fovea region. The CGH interference pattern after our correction is shown in Fig. (5.9). We can see from Fig. (5.9) that the brightness of the interference pattern of the CGH point light source in the peripheral

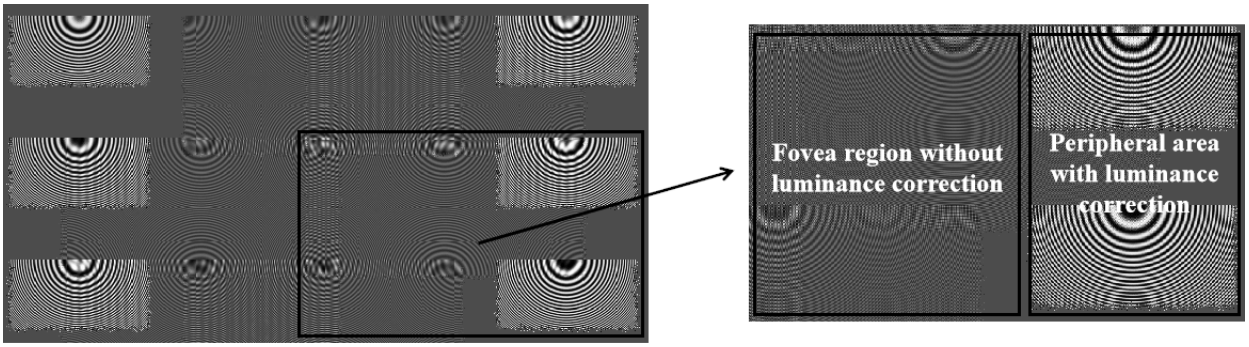


Fig. 5.9 Luminance corrected pattern of CGH

area has been corrected obviously. This is exactly what we bring by correcting the variable a in Eq. (2.1). However, when actually observing the CGH reconstructed image through the digital holography device, we found that the overall luminance of the actual CGH reconstructed image is still slightly lower than the reconstructed image rendered by the CGH conventional method. After discussion, this is most likely due to the overall reduction in diffraction efficiency. Therefore, in order not to affect the observer's viewing of the CGH reconstructed image in the following subjective experiments, I used the darkest reconstructed image as a reference to calibrate the luminance of all the used CGH reconstructed images to ensure the uniformity of the luminance of all images.

5.5.4 Experiment and results for the calculation time

In this section, I will show the comparison between the computation time of my proposed method and CGH conventional method. We can know that the reason for applying foveated rendering to CGH to speed up the calculation speed is mainly due to the following two reasons: 1. In order to reduce the resolution of the peripheral area other than the fovea region, the amount of ray in the peripheral area is reduced, thereby reducing

the calculation amount. 2. In order to fill the gap between the point light sources caused by the reduction in the amount of ray, thereby reducing the calculation amount caused by the reducing of the radius of the zone plate.

Therefore, I calculated the comparison of the calculation time of the overall CGH wave propagation and the calculation time of the Non-foveated (the CGH conventional method) in the case of multiple foveated qualities, as shown in Fig. (5.10). The object I used in the CGH reconstruction image is a checkerboard with 324 points and 162 faces. As shown in the calculation time results in Fig. (5.10), in the case where the foveated quality is the angle of the ray at 0.1 degrees and the radius of the Fresnel zone plate is one-half of the original, we can calculate 1.5 times faster than the CGH conventional method. And, if the field of view is expanded from the current 8 degrees to 30 degrees, we can even get a calculation speed of over 21 times faster than the CGH conventional method. I show the results of the calculation speed of various fields of view in Fig. (5.11).

Based on all the calculation results above, we can know that my proposed method can get a faster calculation speed than the conventional method of CGH, and with the expansion of the field of view, the speed of calculation that my proposed method can achieve is very huge. Therefore, we can conclude that my proposed method is very correct and effective.

5.5.5 Subjective experiment and results

In this section, I will introduce the specific content and results of the subjective experiments. The main purpose of the subjective experiment is to allow the observer to

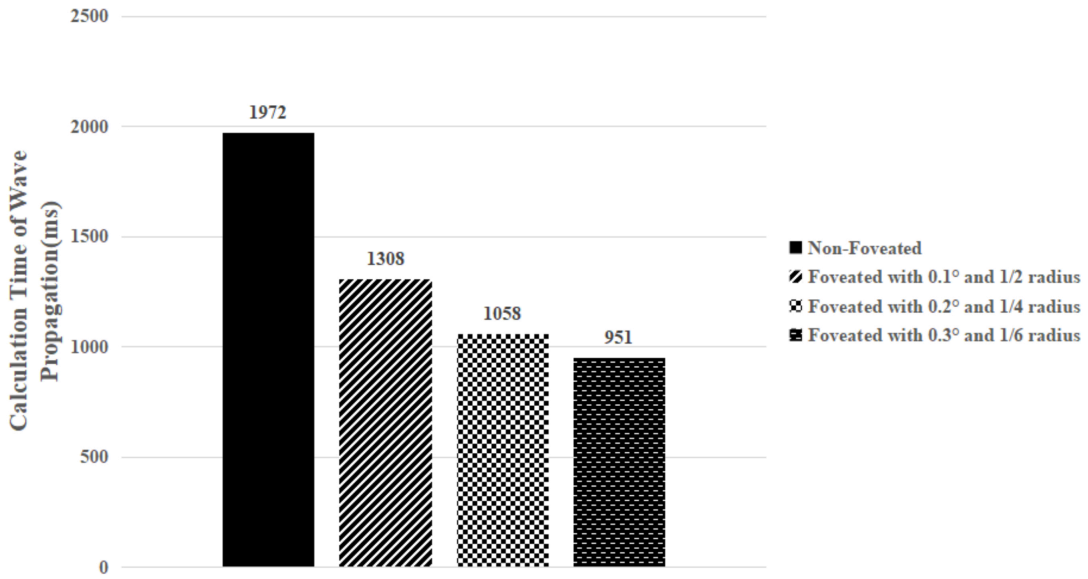


Fig. 5.10 Calculation time of each foveated quality compared with non-foveated rendering

evaluate whether the reconstructed image of the CGH rendered by foveated rendering will affect the observer's viewing. Since all the CGH reconstructed images I used are in the middle of the fovea region, the peripheral area reduces the CGH resolution. Therefore, in actual experiments, the observer needs to focus on the middle part of the image and then evaluate it. Therefore, I invited a total of 12 observers to participate in the subjective experiments. In addition, the subjective experiments are all evaluated based on the pairing experiment, and the final results are all averaged by 12 observers.

This pairing experiment included a total of 3 groups of CGH control groups, and each control group contained a foveated rendering CGH reconstructed image and a non-foveated CGH reconstructed image. I will play each image of each control group for 2 seconds, and between every two control groups, I will insert a pure black screen for 1 second to prevent the observer from being affected by the previous control group when

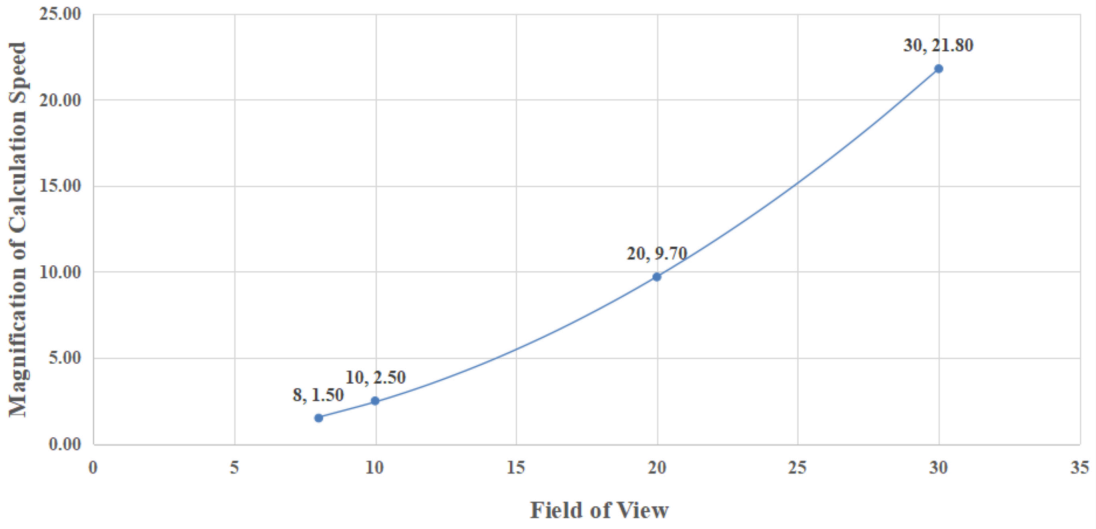


Fig. 5.11 Calculation speed in wider field of view

observing each control group.

In the control group of each group, the non-foveated CGH reconstructed image is an image rendered through a 0.05-degree ray angle, and as a contrast, the reconstructed image of CGH with foveated rendering, I divide its quality q into three grades, q = 3, 2 and 1, where q = 3 is the highest quality, the angle of the ray in the peripheral area is 0.1 degrees, and the radius of the Fresnel zone plate is half of the original radius; q = 2 is medium quality, the angle of ray in the peripheral area is 0.15 degrees, and the radius of the Fresnel zone plate is one-third of the original radius; q = 1 is the lowest quality, the angle of ray in the peripheral area is 0.2 degrees, and the radius of the Fresnel zone plate is a quarter of the original radius. In addition, all the control groups in this pairing experiment will be displayed twice (where the quality q in the order of foveated rendering is from high to low, and from low to high). After each time the observer watches the control group experiment, the observer needs to report the evaluation results

Table 5.3 MOS evaluation

5	Do not mind the difference
4	Not too mind the difference
3	Hard to say on both sides
2	A little mind the difference
1	Mind the difference

to us every time. The evaluation standard used in this experiment is based on the MOS (Mean opinion score) method. I show the evaluation standard in Table. (5.3). Among them, all the evaluations are for the difference between CGH reconstructed images using foveated rendering and non-foveated rendering. I showed some samples about the CGH reconstruction images as shown in Fig. (5.12).

In theory, I should use the angle of ray in the fovea region of 0.017 degrees (the highest resolution limit of the human eye), and the angle of ray of 0.034 degrees in the peripheral area (when the q of foveated rendering is 3). However, because the highest resolution limit of our holographic device is only 0.05 degrees. Therefore, in the final evaluation of the results, since the observer will more or less notice some changes, the average value of the evaluation results will be slightly lower than theoretical. I showed the evaluation results in Fig. (5.13). From the results in Fig. (5.13), we can see that even when the resolution limit of our holographic device is not high enough, we still get an average value higher than 4 when the foveated quality is the highest. Moreover, as the foveated quality of the peripheral area decreases, the average score given by the observer also gradually decreases, which means that as the resolution of the peripheral area decreases, the observers gradually distinguished the difference between foveated rendering and non-foveated rendering, which is also in line with my predictions. There-

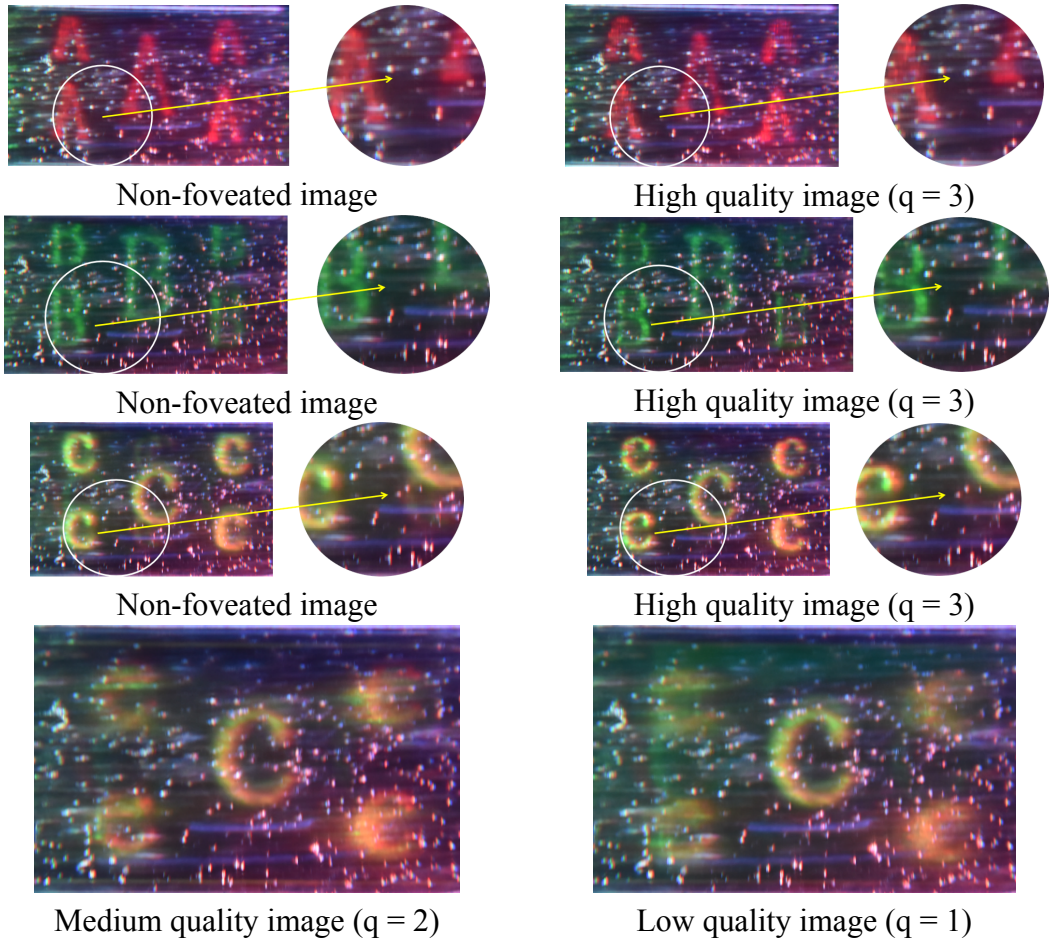
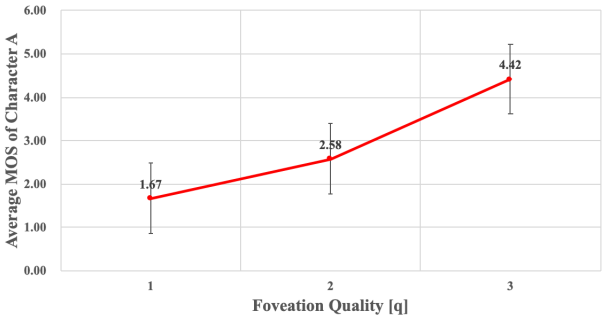
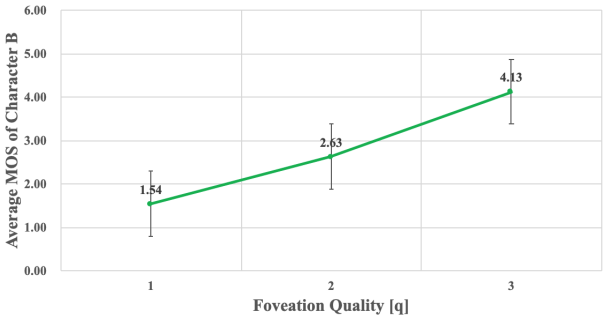


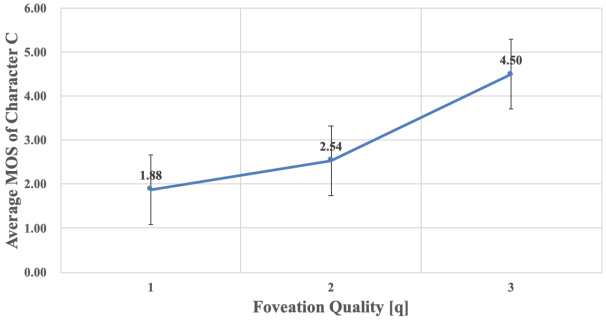
Fig. 5.12 Sample of reconstruction images



Average MOS of character A



Average MOS of character B



Average MOS of character C

Fig. 5.13 Average MOS of characters A, B, and C

fore, from this evaluation result, we can conclude that my proposed method can greatly reduce the calculation amount of CGH and greatly improve the calculation speed of CGH without affecting the observer's viewing of the CGH reconstruction image.

5.5.6 Conclusion for the CGH with foveated rendering

In my proposed method, I provide a new CGH high-speed calculation method using foveated rendering. This method is based on the ray-tracing method, which achieves high-speed calculation of CGH by reducing the number of rays and the radius of the Fresnel zone plate. I have proved through experiments that the relationship between the resolution of CGH and the radius of the Fresnel zone plate; also the relationship

between the luminance of the point light source and the square of the radius of the Fresnel zone plate. And through the measurement of the calculation time, we conclude that under the premise of the 8-degree field of view of our existing holographic device, we have obtained a calculation speed 1.5 times faster than the CGH conventional method. Moreover, as the field of view increases, the calculation speed of my proposed method will become faster. When the field of view is 30 degrees, we can achieve a calculation speed that is 21 times faster than the CGH conventional method. Moreover, through the subjective experiments, we learned that even under the premise that the resolution limit of our existing holographic device is not high enough, we still get an average observer score of greater than 4 in the case of high quality foveated rendering . This also means that in this case, the observer can hardly distinguish the difference between foveated rendering and non-foveated rendering. Although my proposed method is based on traditional holographic device experiments, my proposed method can also be applied to CGH head-mounted display devices. In the future, I will focus on improving the performance of holographic devices, such as increasing the field of view, increasing the resolution limit, and increasing the luminance, etc., to obtain better results for my method.

6

Saccade

6.1 The concept of saccade

Humans have a very wide field of view, and are divided into three main areas as described above: fovea, lateral fovea, and peripheral area. We mainly obtain visual data by the area of the adjacent central fovea, which occupies only 1% of the entire visual field. Although this area only occupies a very small part of the visual field, the information

recorded through this area contains 50% of the effective visual information transmitted to the brain through the optic nerve [50]. Although our outside area vision accuracy is not so good, it is still good at obtaining target movement and contrast information. Therefore, when we focus our eyes on a certain area of an image or an object, we actually put the central fovea area of the eyeball in the area where the lens of our eyeball is currently focused. This shows that due to the visual characteristics of our eyeballs, we will place the most visual processing resources in a specific area of the field of view to obtain the best image. By getting images of the central fovea area, the brain can get the highest resolution images and the most visual data of the area of interest.

The temporal and spatial sampling capabilities of the human eyeball limit how we can extract visual information from our surroundings. As we move our gaze away from the central area of the field of view, the visual accuracy decreases rapidly, so we use a series of eye movements to enable us to place our gaze on the target or scene of interest.

Saccade is a kind of rapid eye movement that moves the fovea region of vision from one point to another, while gaze is to keep the fovea region of vision on the target for a certain period of time to obtain sufficient visual image details. Our visual perception of objects and scenes is accomplished through a series of gazes and saccades. Due to the extremely fast movement of the eyeball when saccade occurs, almost no effective visual information is obtained during this period, and most of the visual information is obtained by gazing. The characteristics of saccades are shown as follows:

- Saccade is a rapid jump from one fixation point to another fixation point. The average time of saccade is about 20-200 ms, and the speed can reach 1000 degrees/second

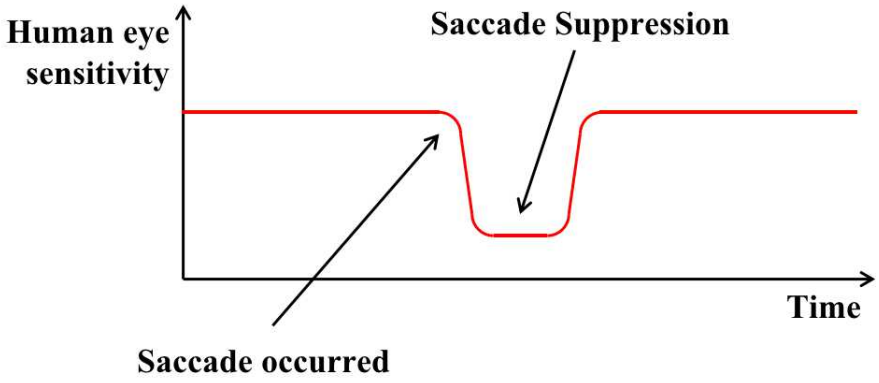


Fig. 6.1 Conceptual figure of saccade suppression

- When reading English, the average saccade is 7-9 letters in length
- The preparation time for making saccades is about 200 ms (delay time); if the saccade distance is large or you need to obtain accurate position information, it takes longer
- Gaze behavior is restricted during saccades
- The end point of saccade cannot be changed during eye movement

After the saccade occurs, the human eye will suppress the visual signals transmitted from the retina to the brain for a period of time. That is to say, after each saccade, our brain hardly feels any visual information from the outside world. This phenomenon is called saccade suppression. The conceptual figure of saccade suppression is shown in Fig. (6.1).

Based on this characteristic of the human eye, since the brain cannot obtain the effective visual information transmitted by the human eye during the saccade, we can use this feature to perform high-speed calculation of CGH. We can detect the movement

of the eyeball through the eye tracking instrument. After the instrument senses that saccade occurs, we can greatly reduce the CGH screen resolution during saccade suppression, which can greatly reduce the amount of calculation required for CGH, thus can make the calculation speed of CGH greatly improved, and because the human eye cannot perceive the external visual information during saccade suppression, my method to reduce the resolution of the CGH reconstruction image will not have any bad effect on the observer watching the CGH.

6.2 Some applications of saccade suppression

In the previous section, we already know that when the human eye occurs saccade, the external visual information will not be transmitted to the brain through our retina. We call this phenomenon saccade suppression. Regarding the application of saccade suppression, in the field of CG, there have been many researches published about the using of this phenomenon of human eyes to realize a fast calculation for head-mounted display devices. One of the researches is about using the human eye's saccade suppression phenomenon to create a virtual world that is wider than the real world for users of head-mounted display devices to obtain a better VR experience [51].

The main principle of this technique is that when saccade occurs in the human eye, saccade will last for a period of time. During this time, it can use the principle of saccade suppression to rotate or move the VR world a little. The direction and distance of the user's movement in the real world are determined based on the scenery they see in the VR world. Therefore, when the user occurs saccade, this method can slightly rotate or move the scenery of the VR world, so that the user can rotate the distance or direction of

their movement in the real world without perceiving any abnormalities. Although this rotation and movement is very small during a saccade (in order not to let users notice the obvious rotation and movement in the VR world), as multiple saccades occur, the amount of this rotation and movement can be accumulated continuously. In this way, when users experience the VR world, when an obstacle appears in front of them (such as a chair, a wall, etc.), they can constantly change the VR world through sensors on the head-mounted display device. Therefore, the user can bypass the obstacle without affecting the user experience in the VR world, and also avoids the user from hitting the obstacle because he cannot see the appearance of the real world. Based on this solution, the size of the world that users can actually experience in the VR world can be wider than the size of the real world. In addition, these sensors and the changes in the VR world are calculated and rendered in real time by the GPU. In this way, it is possible to avoid a sudden presence of an obstacle in the user's travel path, which is too late to react. Although it is still in the research stage, it can be used even if the user does not understand the function, and it can be used regardless of the content type, so it is very likely to be put into practical use and mass production.

Based on this research, we can clearly know that when saccade occurs in the human eye, the brain really cannot obtain any external visual information from the retina. Therefore, it is achievable to use the phenomenon of saccade suppression to reduce the calculation amount of CGH and greatly increase the calculation speed of CGH.

7

CGH high-speed calculation using saccade suppression

In the previous chapter, I have introduced in detail the background of foveated rendering and how to apply foveated rendering to the high-speed calculation of CGH. Since the resolution of the human eye in the peripheral area other than 5 degrees of the gaze area

will be greatly reduced, why do we not particularly perceive the surrounding world as blurred when viewing the surrounding scenery? This reason is actually because the human eye is moving rapidly in daily life all the time, and we call this human eye movement saccade.

In the previous chapter, I have introduced some characteristics of saccade and some applications in other fields. As I introduced, saccade is a rapid movement of the human eye. It usually occurs when the human eye switches gazing objects (whether the human eye actively switches gazing objects or passively occurs due to external stimuli), such as observing the scenery, reading and playing games, etc. Therefore, in this chapter, I will give you a detailed introduction to my second proposed method, the CGH high-speed calculation using saccade suppression.

7.1 Overview of the proposed method using saccade suppression

The human eye will generate a saccade because it actively switches the gazing scene or passively switches the gaze scene due to external stimuli. When the saccade happened, our brain hardly received any external visual information from the retina, and we call this phenomenon saccade suppression. This phenomenon has been used in the field of VR to expand the size of the VR world and avoid obstacles in time. This successful application strongly proves the feasibility of using saccade suppression to optimize algorithms in the field of VR. Therefore, I decided to apply this feature of the human eye to CGH to optimize the algorithm of CGH, reduce the amount of CGH calculation, and thus increase the speed of CGH calculation.

As we know, one of the disadvantages of CGH is that it is very computationally

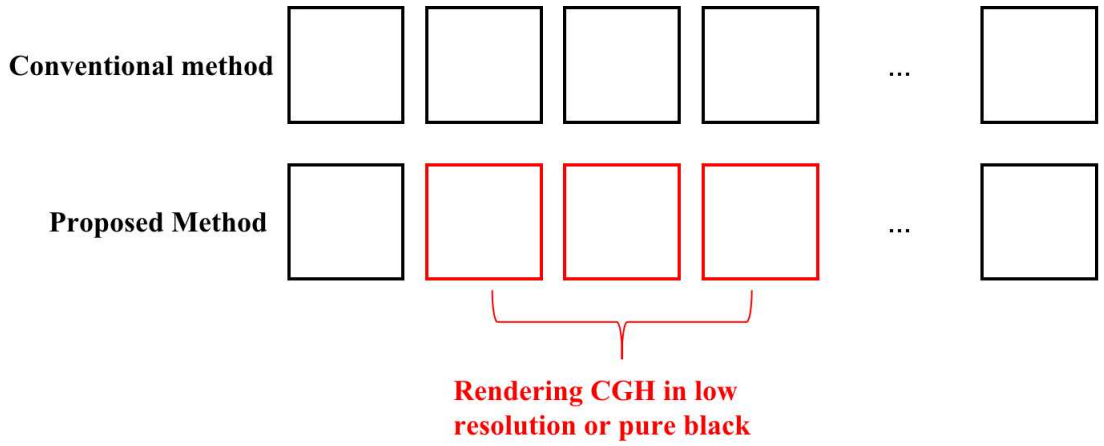


Fig. 7.1 CGH fast calculation with saccade suppression

intensive, and the human eye often happens saccade in daily life, and during the saccade, the human eye cannot perceive the external visual information. Since the human eye cannot perceive the visual information of the outside world, we can use this time to greatly reduce the resolution of the CGH screen during saccade suppression, or even not render at all, and directly output the pure black screen to achieve the purpose of greatly reducing the amount of CGH calculation. The specific implementation is shown in Fig. (7.1). As shown in Fig. (7.1), the red area is the period during which saccade occurs. I first detect the occurrence of saccade. During the subsequent saccade suppression, I greatly reduce the resolution of CGH or directly output pure black images to reduce the amount of calculation of CGH. In this way, we can achieve high-speed calculation of CGH.

7.2 Human reaction time

As I mentioned in the last section, under ideal conditions, I will reduce the resolution of the CGH reconstruction image after detecting the occurrence of saccade in the human eye or do not perform any rendering to reduce the amount of CGH calculation. But in fact, even if the human eye's saccade will last for hundreds of milliseconds, due to the huge amount of current CGH calculation, even if we have detected that after the occurrence of saccade, we still cannot reduce the resolution of CGH in real time. Therefore, we need to change to another way to implement my proposed method. As I mentioned before, the human eye will induce saccade due to external stimuli. Therefore, we can pre-render several sets of CGH animations. In the animation, we can make the objects inside jump around randomly, thereby inducing the saccade of the human eye. And after each jumping, I reduce the resolution of CGH or directly output the pure black image, and then let the observer determine whether any abnormalities are felt when watching the CGH animation, so as to make sure whether my proposed method is effective or not.

However, for humans, it takes a certain reaction time for external stimuli. For example, the athlete starts running after hearing the sound of the starting gun, the driver brakes after seeing the obstacle, etc. Similarly, it takes a certain reaction time for the observer to watch the random jumping motion of the object before the saccade occurs. Therefore, if we take human reaction time into consider, my proposed method can be represented in Fig. (7.2). From Fig. (7.2), we can see that after the random jump motion of the object, within the human reaction time, we need to continue to render the CGH

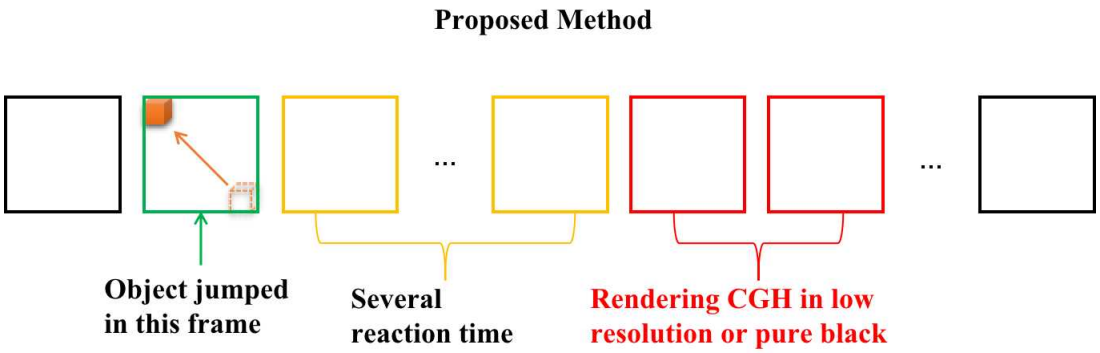


Fig. 7.2 CGH fast calculation with saccade suppression and reaction time

at the original resolution for several frames, and then reduce the CGH resolution during the subsequent saccade suppression. In this way, I can make my proposed method more reasonable, and will not let the observer feel any abnormality to the CGH animation.

7.3 Duration time of saccade suppression

In the previous section, I introduced the concept of human reaction time, and took this concept into my proposed method and optimized it. However, because we must accurately control the duration time of the CGH animation resolution reduction within the duration time of saccade suppression. Therefore, we must know the length of saccade suppression beforehand, in order to accurately know how many frames the resolution should be reduced during pre-rendering. Regarding the question of the length of saccade suppression, there have been many discussions on this issue in previous researches. After the review, in reference [52], I found a very representative conclusion. The literature points out that for human saccade suppression, its duration time is very fixed, and very easy to measure. Because numerous researches have proved that the duration time of human saccade suppression has a nearly perfect linear relationship with the angle of

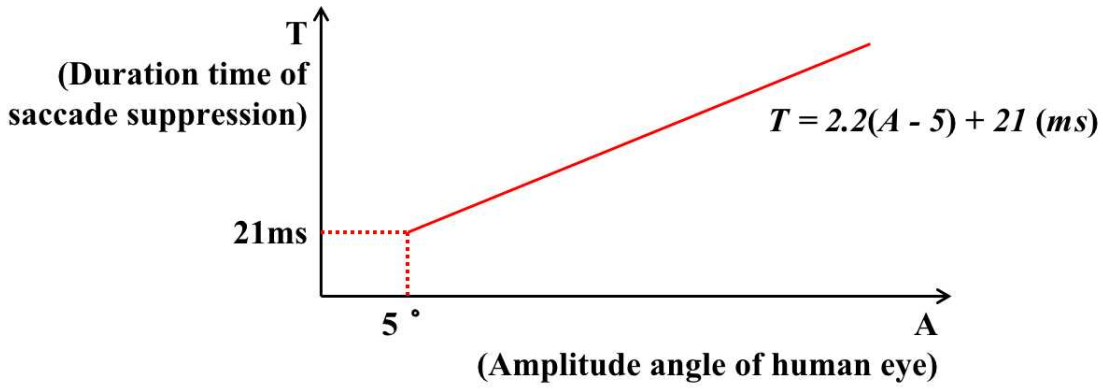


Fig. 7.3 The relationship between duration time of saccade suppression and amplitude angle of human eye

amplitude of human eyes. The Eq. (7.1) shows the relationship between the duration time of saccade suppression and the amplitude of human eye which is defined as

$$T = 2.2(A - 5) + 21(ms). \tag{7.1}$$

In this Eq. (7.1), T represents the duration time of saccade suppression, and A represents the amplitude angle of the human eye (where A must be greater than 5 degrees). Therefore, based on this Eq. (7.1), we can get the conclusion which is shown in Fig. (7.3).

Based on this conclusion, we can easily calculate the amplitude angle of the human eye according to the angle at which the object jumps. Therefore, we can know the specific duration time of saccade suppression, which can accurately control the length of time that the resolution of CGH animation is reduced, so that the observer will not feel any abnormalities when watching CGH animation.

7.4 High-speed calculation of CGH based on saccade suppression

The previous sections have introduced some points that need to be paid attention to when applying saccade suppression to the field of CGH in detail. Therefore, in this section I will introduce several reasons about why my proposed method can perform high-speed calculations. My proposed method can perform high-speed calculations mainly for the following three reasons: 1. The reduction in the number of rays caused by lowering the CGH resolution. 2. The reduction of the radius of the Fresnel zone plate due to the reduction of resolution. 3. The frequency of saccade and the duration time of saccade suppression.

First, for the high-speed calculation of the first and second points, the basic principles are similar to those described from Eq. (5.6) to Eq. (5.12) which can be defined as

$$O(L^4 r_S^4), \tag{7.2}$$

or defined as

$$O(\frac{L^4}{\vartheta_S^4}). \tag{7.3}$$

In Eq. (7.2) and Eq. (7.3), L represents the size of the hologram, r_S represents the radius of the Fresnel zone plate, and ϑ_S represents the angle of ray. Also, we summarized the reasons for these two points into Fig. (7.4) and Fig. (7.5). Therefore, if we reduce the radius of the Fresnel zone plate and increase the angle of the ray, the computational complexity will be reduced to the fourth power of the amount of change.

The third reason that allows my proposed method to perform high-speed calculations is that saccade often occurs in the human eye, and after each saccade, saccade

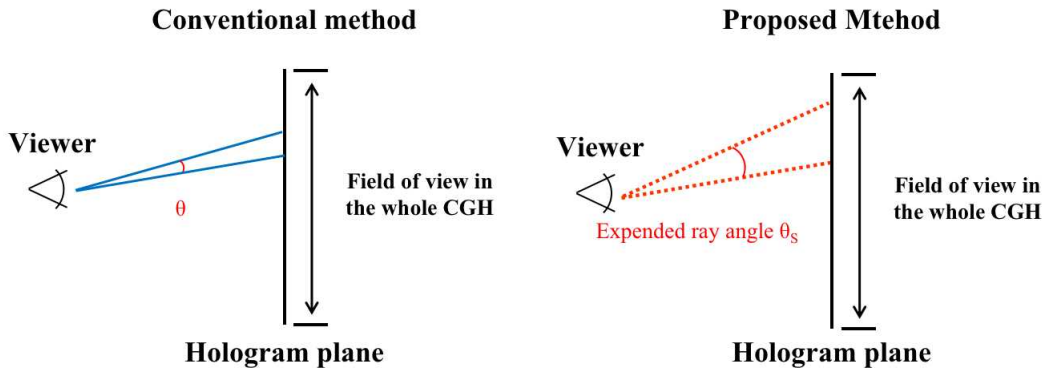


Fig. 7.4 Expand the ray angle

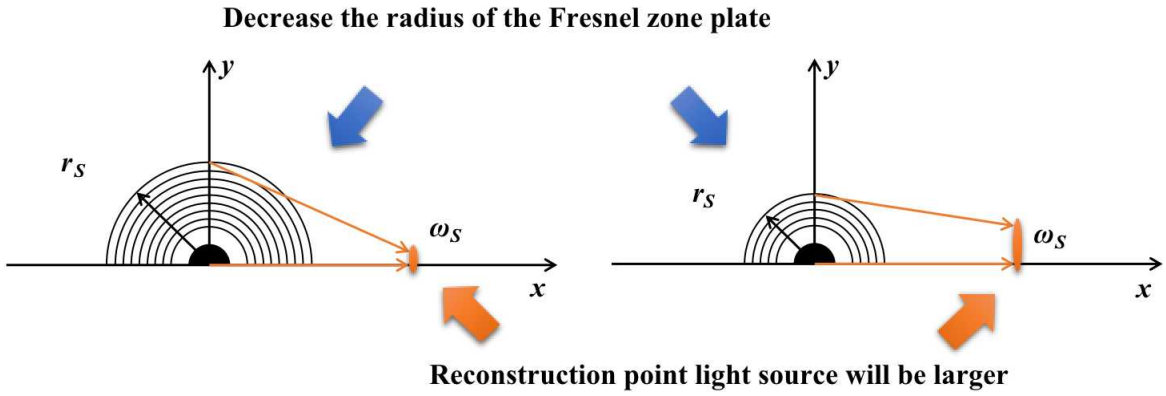


Fig. 7.5 Reduce the radius of Fresnel zone plate

suppression will continue for a period of time, so that we can continuously reduce the resolution of CGH to greatly reduce the amount of calculate, and increase the calculation speed without affecting the observer watching CGH animation. Therefore, for this reason, we can summarized into the following equation which is defined as

$$S \propto fT. \tag{7.4}$$

In this Eq. (7.4), S represents the calculation speed of CGH, f represents the fre-

quency of saccade (the human eye is usually 2-8 times per second), and T represents the duration time of each saccade suppression. From Eq. (7.4), we can see that as the frequency of saccade increases and the duration time of each saccade suppression increases, the overall calculation speed of CGH will be greatly improved. Finally, we concluded the reasons for the three-point high-speed calculation into the following equation which can be defined as

$$S \propto \frac{fT}{O}. \tag{7.5}$$

The O in the Eq. (7.5) is the computational complexity derived from Eq. (7.2) and Eq. (7.3). Due to this Eq. (7.5), we can clearly understand that based on the above three reasons, my proposed method can achieve high-speed calculation of CGH, and will not affect the observer watching CGH animation.

7.5 Experiments and results for CGH with saccade suppression

7.5.1 Experimental environment and devices for CGH with saccade suppression

Next, I will introduce the experimental design and experimental results of my second proposed method. The experimental content of my second proposed method mainly includes two parts. The first part is the subjective experiment design and observer evaluation, and the second part is the calculation time comparison with the CGH conventional method. The detailed parameters of the computer and the detailed parameters and appearance of the holographic device used in the experiment are shown in Table. (7.1), Table. (7.2), Fig. (7.6) and Fig. (7.7). We can see that in Fig. (7.6) and Fig. (7.7), except the traditional holographic device, I also connected a device called ET-

Table 7.1 Parameters of computer for CGH with saccade suppression

CPU	Intel Core(TM) i9-7900X
OS	Windows 10 Professional 64 Bit
RAM	32.0 [GB]
Clock Frequency	3.30 [GHz]
GPU	NVIDIA GeForce GTX 1080Ti

Table 7.2 Parameters of holographic display for CGH with saccade suppression

Pixel pitch of SLM	6.4×6.4 [μm]
Number of pixel	1,920×1,080 [pixels]
Resolution limit	0.034°
Angle of Field of View	11.1° [H] x 6.2°[V]
Wavelength of each color	Red:625 [nm] Green:525 [nm] Blue:465 [nm]

3D10, which is the device I use to detect the eye movement of the observer. Through this device, we can clearly see the time point of the observer's saccade. Therefore, the observer must observe and evaluate the CGH animation through ET-3D10 when conducting subjective experiments. Also, all the CGH calculation is using our computer by GPU [53].

7.5.2 Design of the subjective experiments

In this section, I will introduce the design of the subjective experiments in detail. In the previous, I have introduced that when conducting subjective experiments, I will pre-render several kinds of CGH animations. The contents of the animation include random jumping movements of objects at different time points. Therefore, before the subjective experiment begins, I will need to pre-render the used CGH animation. In addition, each animation is produced and rendered at a frame rate of 60 FPS and 12 seconds duration time. Each animation includes random jumping movements of objects

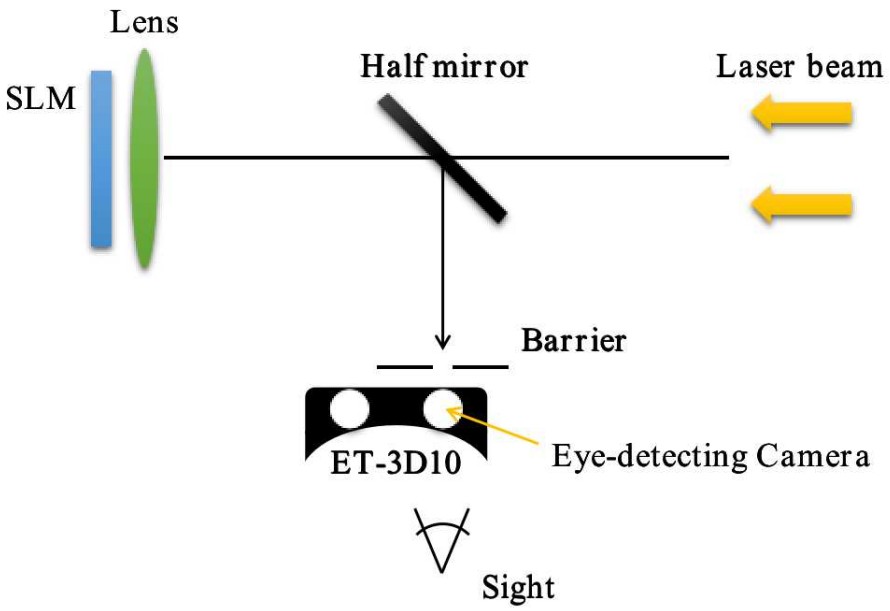


Fig. 7.6 Holographic device for CGH with saccade suppression in concept

at different time points, and the jumping movements of the objects in each animation is totally five times. I show one of the CGH animations as an example in Fig. (7.8). In addition, all pre-rendered CGH animations will be divided into three groups, which is classified as the resolution of CGH during the saccade suppression be reduced to 0% (which means output a pure black image without any light wave information of point light source, so the calculation time is 0), 10% and 30%. I show an example of reducing the CGH resolution in Fig. (7.9). After the observer has watched all the CGH animations, the observer needs to report to us how many times the anomaly of is seen in each animation (such as screen flicker, screen blur, screen disappear, etc.). After that, I will make a final score for the CGH animation based on the observer 's report. The score is based on the total score of 5 points minus the number of times the observer reported the abnormality. For example, when the observer reports that he felt the abnormality of

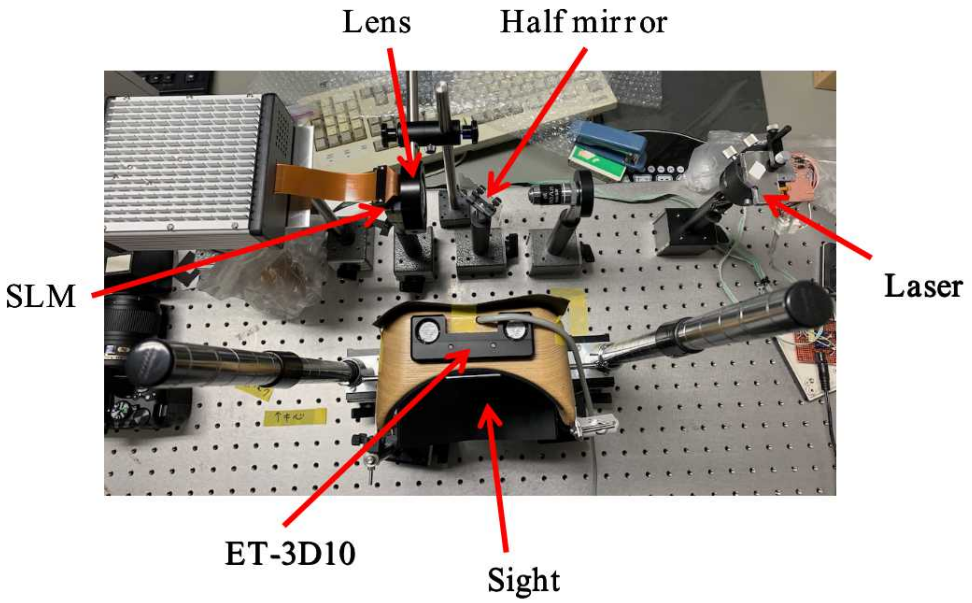
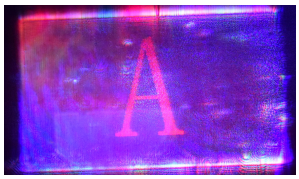


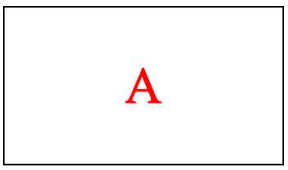
Fig. 7.7 Holographic device for CGH with saccade suppression in real

the screen twice, we subtracted 2 from 5 according to the report result, and finally got 3 points, which is the final score of the CGH animation. A detailed description of the final score is shown in Table. (7.3).

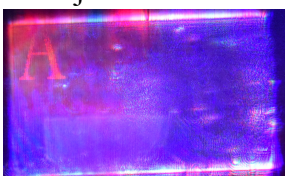
Another thing we need to pay attention to is that we know that human response to external stimuli requires a reaction time, and for the average person, the average response time is 0.2 seconds (this means that in my 60 FPS CGH animation, it will last about 12 frames. And I will also call this period "delay frame"). Therefore, when we pre-render the CGH animation, we must consider this average reaction time, and add this delay frame when the object jumps randomly, and then reduce the resolution of the CGH animation. Although we already know that for the average person, the average human reaction time is 0.2 seconds (12 delay frame), but for the individual observer, there will be an individual difference in the reaction time of each person. Therefore, in



Object in middle



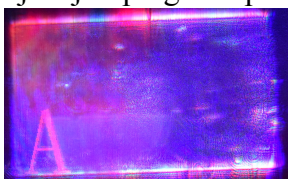
Object in middle



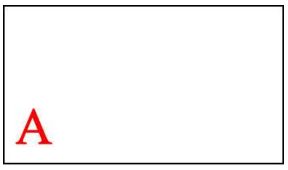
Object jumping to top left



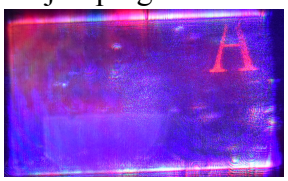
Object jumping to top left



Object jumping to bottom left



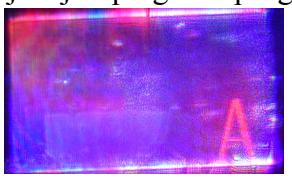
Object jumping to bottom left



Object jumping to top right



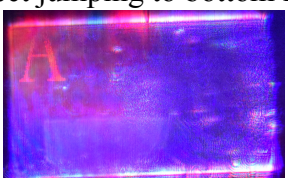
Object jumping to top right



Object jumping to bottom right



Object jumping to bottom right

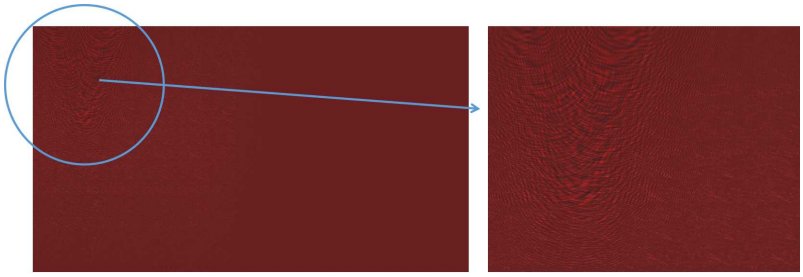


Object jumping to top left

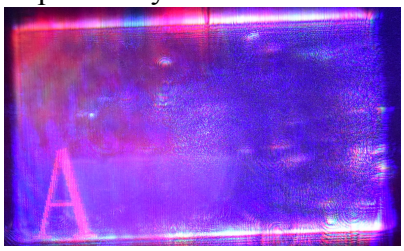


Object jumping to top left

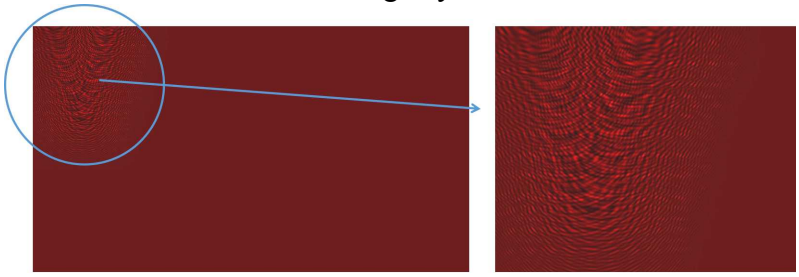
Fig. 7.8 Example of the jumping motion of object



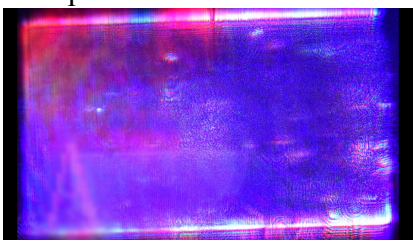
CGH pattern by conventional method



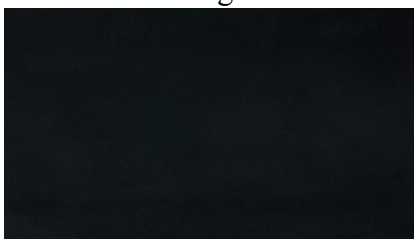
CGH reconstruction image by conventional method



CGH pattern with 30% resolution



CGH reconstruction image with 30% resolution



CGH pattern with 0% resolution (nothing is rendered, pure black)

Fig. 7.9 Example of the patterns and reconstruction images of reducing CGH resolution

Table 7.3 Details about the evaluation

Score	Quality of CGH animation
5	Do not have any unusual feeling
4	Experienced one time of unusual feelings
3	Experienced two times of unusual feelings
2	Experienced three times of unusual feelings
1	Experienced four times of unusual feelings
0	Experienced five times of unusual feelings

the subjective experiment, I decided to extend the reaction time to a range of 0.1 seconds to 0.3 seconds (approximately 6 delay frames to 17 delay frames). In summary, I have prepared three groups of CGH animations, respectively, during the saccade suppression period, the CGH resolution is reduced to 0%, 10% and 30%. Based on the human reaction time, I subdivided the CGH animation into 12 groups in each large group, representing 12 categories of delay frames from 6 to 17. Therefore, for each observer, it is necessary to watch a total of 3 x 12 groups, a total of 36 groups of CGH animations, and evaluate all 36 groups of animations.

7.5.3 Results for the subjective experiment

Next, in this section, I will show all the results of the subjective experiments in detail. In the subjective experiment, I invited a total of 20 observers to participate in the subjective experiment, aged between 19 and 22 years old. However, for some reasons, in the final result statistics, a total of 5 observers misunderstood the content of the experiment and gave wrong evaluation results. Therefore, when I finally summed up the evaluation results of the subjective experiments, I removed the experimental results of these 5 observers, and finally took the average of the data of the remaining 15 observers as the

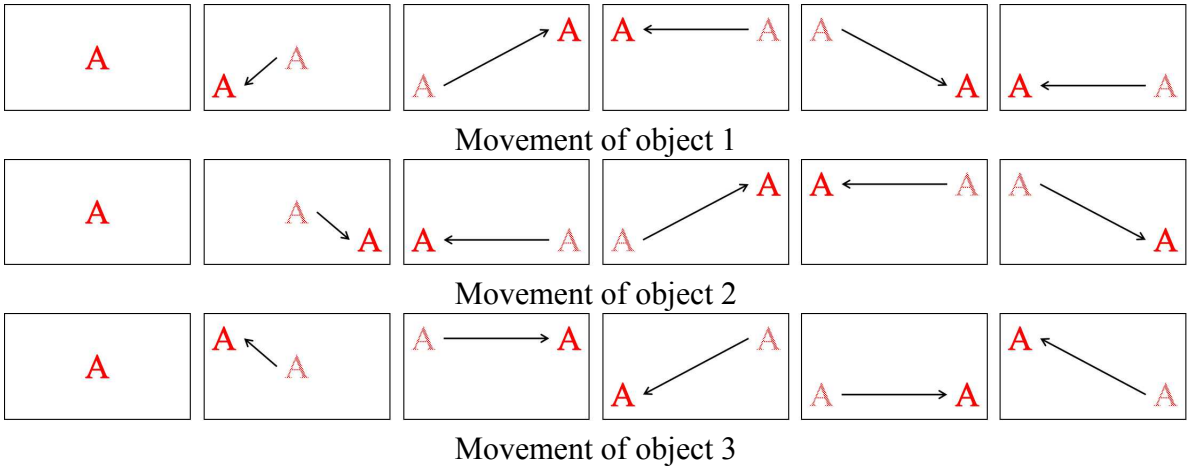


Fig. 7.10 Movement of the object in different types of CGH animations

final evaluation results.

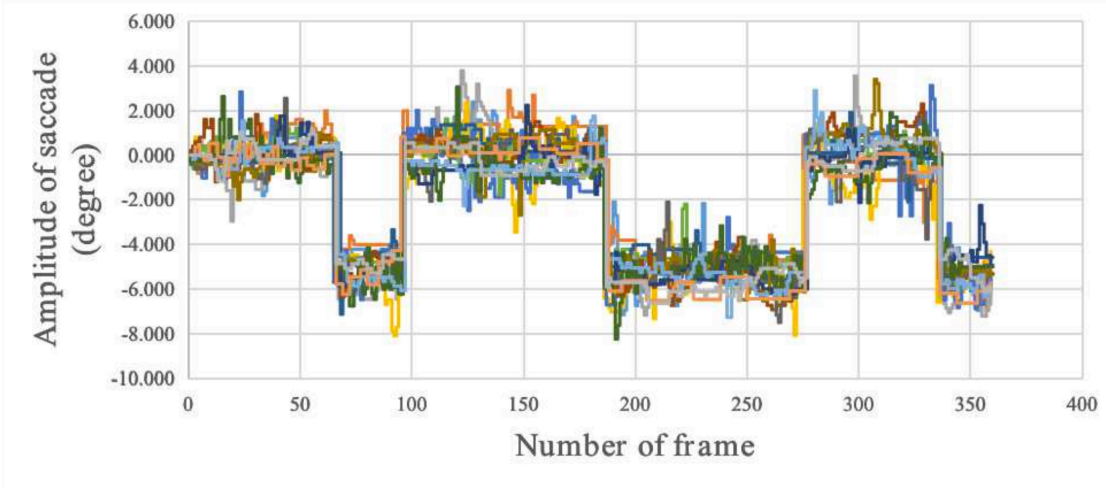
In order to ensure that all observers have the saccade correctly at the right time, I assembled and connected our holographic device with the ET-3D10 device to ensure that the motion of eyeballs of each observer were recorded throughout the experiment and the ET-3D10 device detects eye movement at a frequency of 30 Hz. In 12 different delay frame CGH animations, I generated 12 kinds of the movement of object, each contains an object that jumps in different directions at different points in time, and I show three examples for the movement of objects in 12 different delay frame CGH animations in Fig. (7.10).

I show three results of the observer's eye movement recorded by ET-3D10 in Fig. (7.11). The axis of abscissa represents the number of frames of the eye movement recorded by ET-3D10 during the 12-second CGH animation (based on the 30 Hz sampling rate of ET-3D10), and the axis of ordinate represents the amplitude angle of the movement of the eyeball. In Fig. (7.11), we can see that all observers have correctly

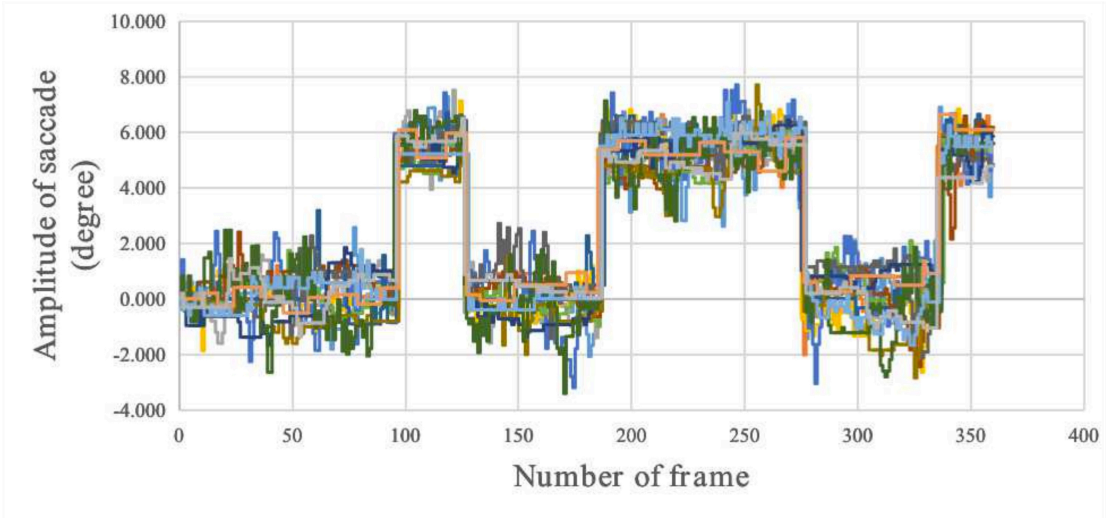
observed the motion of the object at the correct time point, and the saccade has occurred correctly (where the amplitude angle of the eyeball has changed significantly). And the time point of occurrence of saccade for 15 observers are very similar, which also proves that the reaction time of 15 observers is about 0.2 seconds (12 delay frames).

Next, I will show the evaluation results of the subjective experiment. Fig. (7.12) shows the average value of the observer's evaluation of all CGH animations in detail. From the results in Fig. (7.12), we can see that I set the response time in the range of 0.1 seconds to 0.3 seconds, which is 6 to 17 delay frame. In the case of different delay frames, observers also have different evaluation results on whether they can feel abnormalities in the CGH animation. At 12 delay frame (which is 0.2 seconds reaction time), no matter what resolution the CGH is reduced to during the saccade suppression, the average evaluation result is 4 points or more, which means that the observer can hardly notice any abnormal when watching the CGH animation. And as the delay frame is set to be greater than or less than 12 delay frame, the average evaluation result of CGH animation has a downward trend, which also meets my expectations for the result. As the setting of the response time deviates from the 12 delay frame of the average value, the reduction of the resolution of the CGH animation will gradually be inconsistent with the occurrence of saccade suppression of the human eye, so the observer will inevitably have more unusual feelings in the CGH animation.

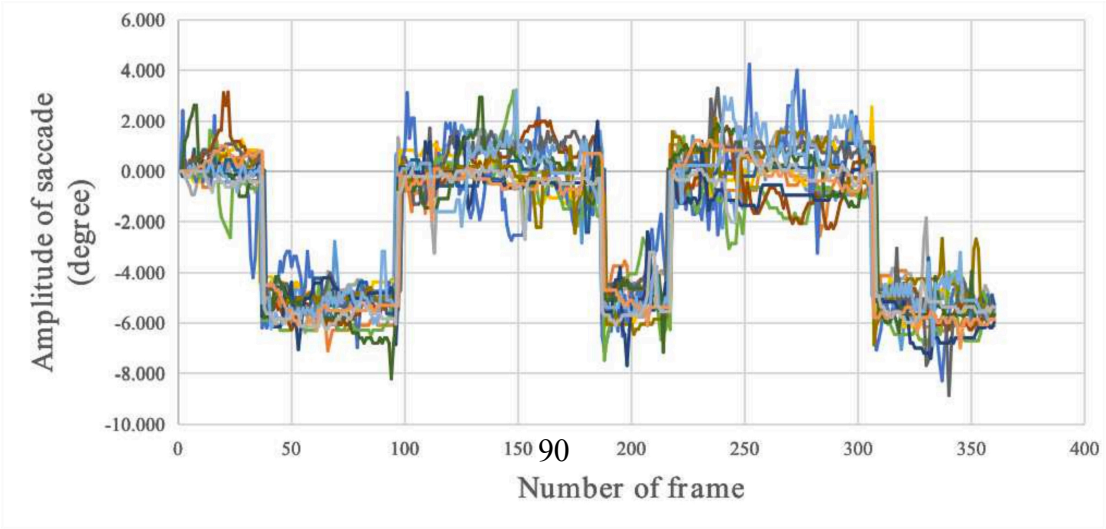
Moreover, in the results of Fig. (7.12), we can also see that when the delay frame is set between 8 and 9, or 14 and 15, the average evaluation result of the 30% CGH animation resolution is higher than other two resolutions of CGH animation. Therefore, I did t-Test for these situations. The results of t-Test are shown in Table. (7.4). From



Saccade category 1



Saccade category 2



Saccade category 3

Fig. 7.11 Part of results of the saccade

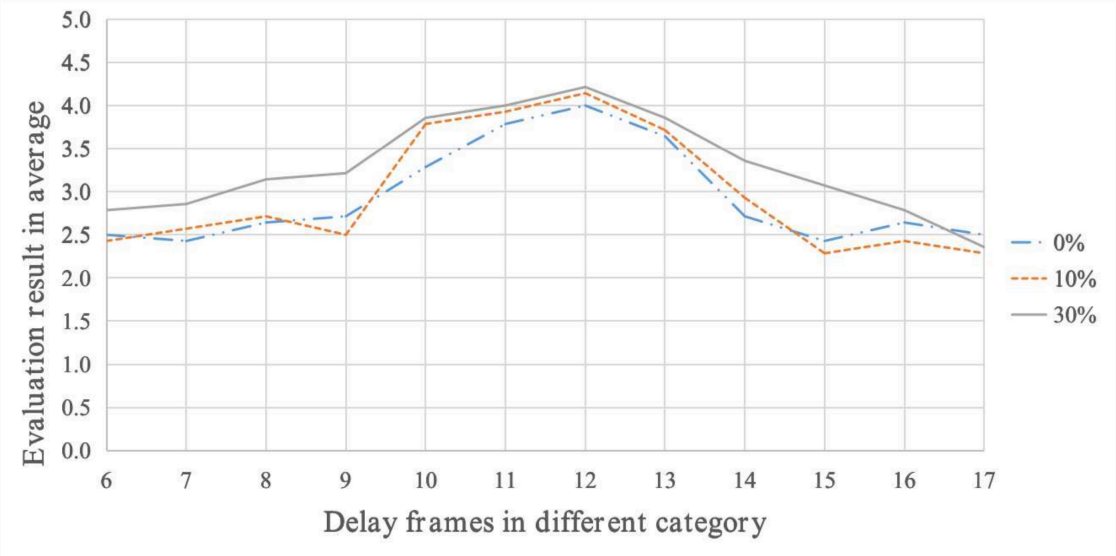


Fig. 7.12 Evaluation result in average

Table. (7.4), we can see that in the case where the delay frame is 9, the result of the 30% resolution CGH animation is significantly higher than the other two resolution CGH animations. In the case of the other three delay frames, although the t-Test result does not yield significance, the average evaluation result of the 30% resolution CGH animation is still higher than 3, which means that in 5 times random motion of an object, the observers can only have unusual feelings within 2 times. Therefore, in practical applications, I still believe that 30% resolution CGH animation will perform better than the other two.

Based on all the above results, we have concluded that when the delay frame is set properly, the observer cannot feel the decrease in CGH animation resolution during saccade suppression.

Table 7.4 Results of t-Test

Content of t-Test	Value
30%-8 delay frames to 0%-8 delay frames	0.14
30%-9 delay frames to 0%-9 delay frames	0.09
30%-14 delay frames to 0%-14 delay frames	0.10
30%-15 delay frames to 0%-15 delay frames	0.13
30%-8 delay frames to 10%-8 delay frames	0.19
30%-9 delay frames to 10%-9 delay frames	0.04
30%-14 delay frames to 10%-14 delay frames	0.22
30%-15 delay frames to 10%-15 delay frames	0.08

7.5.4 Results for the calculation time

Finally, I will calculate and compare the calculation time of my proposed method with the CGH conventional method. For the calculation of the calculation time, I will mainly divide the following two parts for comparison: 1. Comparing the calculation time of the CGH reconstructed image after the single-resolution reduction. 2. Comparison of the calculation time for the overall CGH animation.

First I will show a comparison of the calculation time for the first part. Fig. (7.13) shows a detailed comparison of the calculation time. In Fig. (7.13), we can see that I have measured the calculation time for character A at multiple resolutions. In the CGH conventional method, I set the angle of ray to 0.034 degrees. Therefore, the 30% resolution CGH reconstructed image has an angle of ray of 0.11 degrees, while the 10% resolution CGH reconstructed image has an angle of ray of 0.34 degrees. From the results of calculation time, we can see that in the situation of the 30% resolution of the CGH reconstructed image, we can get a calculation speed increase of more than 4 times, while the resolution of the reconstructed image on the CGH is 10%, we can

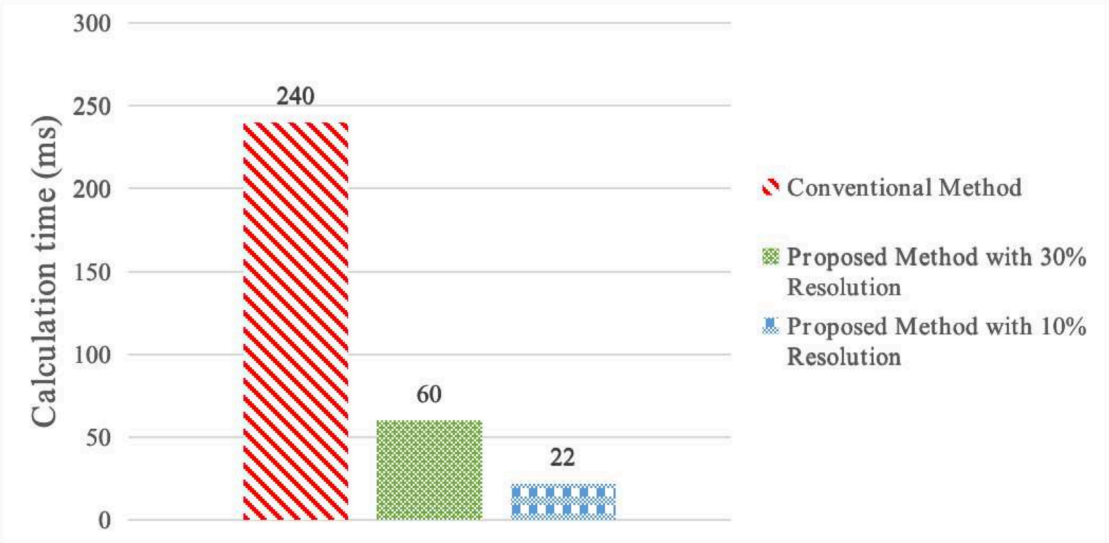


Fig. 7.13 Calculation time of Character A

get more than 10 times improve the speed of calculation. Although in the experiment of comparing the calculation time, I only used relatively simple objects for the calculation, but based on references [54, 55], we can still get an approximate increase in calculation speed.

Next, I will show a comparison between the overall calculation speed of CGH animations. For the overall calculation speed of CGH animation, the main improvement is the number of saccade occurrences and the length of time for each saccade suppression. Therefore, I show the relevant results in Fig. (7.14). In Fig. (7.14), we can see that as the number of occurrences of saccade increases and the length of time for saccade suppression increases, compared to the CGH conventional method, the computation speed of my proposed method will become faster and faster. In our daily life, the frequency of saccade is about 2 - 8 times per second, and the duration time of each saccade suppression is generally between 20 - 200 milliseconds. Therefore, for my CGH animation

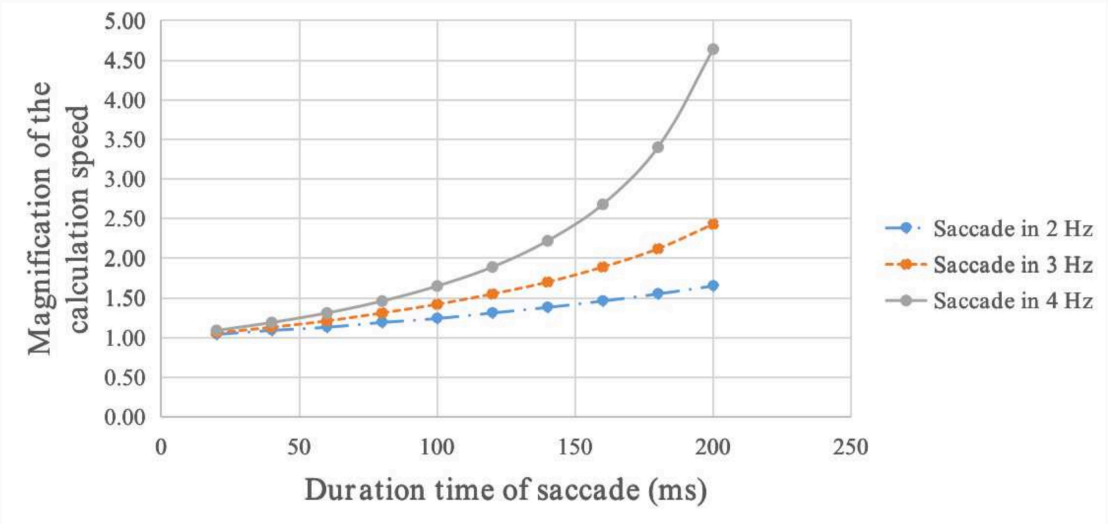


Fig. 7.14 Calculation speed

with a frame rate of 60 FPS, at the frequency of 4 times per second of saccade, when the duration time of saccade suppression is 200 milliseconds, my proposed method for the overall calculation speed of CGH animation should is 4.64 times faster than the calculation speed of CGH conventional method.

Based on the above calculation time and speed measurement, we can conclude that my proposed method can use saccade suppression to perform high-speed calculation of CGH, and will not have any bad impact on the viewer watching CGH animation.

7.5.5 Conclusion for the CGH with saccade suppression

In my second proposed method, I developed a new CGH high-speed calculation method, using saccade suppression to perform high-speed calculation of CGH. Through the subjective experiments, I set different delay frames and different CGH resolutions during the saccade suppression to allow our observers to evaluate the CGH animations in turn.

From the results, we can know that when the delay frame setting is just right (12 delay frames), no matter how the resolution of the CGH is reduced, the observer can hardly notice any abnormality of the CGH animation. In the delay frame between 8 to 9 and 14 to 15, I prefer to use a 30% CGH resolution reduction to achieve better results. Through the measurement of the calculation time and calculation speed, we have obtained that in the case of a single CGH reconstructed image, a 30% resolution reduction can achieve more than 4 times high-speed calculation, while 10% resolution can achieve a high-speed calculations for over 10 times. In terms of the overall calculation speed for CGH animation, when the frequency of saccade is 4 times per second and the duration time of saccade suppression is 200 ms, we can achieve 4.64 times of high-speed calculation. Therefore, we can conclude that my CGH high-speed calculation using saccade suppression can achieve the purpose of CGH high-speed calculation without affecting the observer watching CGH animation.

8

Discussion and summary

In this thesis, I provide two high-speed calculation methods for CGH: 1. CGH high-speed calculation method using foveated rendering. 2. CGH high-speed calculation method using saccade suppression.

I first introduced the details of foveated rendering and related applications in the field of CG. Then introduced another feature of human eyes closely related to foveated

rendering, saccade and saccade suppression. Then, I made a detailed discussion about the application of foveated rendering in the field of CGH, and proposed a method to solve the reduction of CGH resolution, the relationship between point light sources and Fresnel zone plate. Subsequently, I elaborated on the principle of high-speed calculation of CGH after using foveated rendering for the characteristics brought after applying foveated rendering to CGH. Second, I introduced the principles of saccade about the human eye and the characteristics of saccade suppression that occurred during saccade. And for the characteristics of saccade suppression, I put forward another theoretical basis for CGH's high-speed calculation. Using the previous CGH resolution reduction, point light source and Fresnel zone plate theory, I verified the feasibility of using saccade suppression for CGH high-speed calculation and made a detailed analysis. Finally, through various theoretical experiments and subjective experiments, I objectively and comprehensively verified the validity and correctness of my two proposed methods. On the basis of actual data, once again proved the feasibility of foveated rendering and saccade suppression used in CGH.

Through my first experiment, we learned that without affecting the observer's viewing of CGH and reconstructing the image, I use foveated rendering to bring 1.5 times the calculation speed of CGH on our existing holographic device, and when the field of view is expanded to 30 degrees, we can get more than 21 times the speed of the calculation. Through my second experiment, we can know that for a single CGH reconstructed image, after reducing the resolution to 30%, we can get more than 4 times the calculation speed, and after reducing the resolution to 10%, we can get more than 10 times the calculation speed. For CGH animations, when saccade occurs at a frequency of 4 per

second and saccade suppression is 200 milliseconds, we can get an overall 4.64 times increase in the computational speed of CGH animations. Therefore, we can conclude that for my two proposed methods, after being applied in the field of CGH, the calculation speed of CGH can be greatly improved without affecting the observer watching CGH.

In the future, I will focus on studying the fusion of these two human eye features about the foveated rendering and saccade suppression or more to increase the speed of CGH calculation. This will have a profound and significant impact on the most ideal 3D imaging technology, which is the computer-generated holographic technology for the real-time calculation.

Acknowledgments

I sincerely thank my instructor, Professor Yuji Sakamoto, for his continued support for my doctoral research and related research. Thank him for his patient teaching and rich knowledge. Under his guidance, I have been conducting research and writing this thesis during my Ph.D. I would also like to thank my Collaborator Professor Fumio Okuyama, thank him for his comments and suggestions on my research, which benefited me a lot.

In addition to my instructor and collaborator professor, I would also like to thank other deputy instructors: Professor Kenji Araki, Professor Miki Haseyama and Associate Professor Yoshinori Dobashi. Their rich insights and encouragement also inspired me to continue to solve all the difficult problems in the research, allowing me to carry out my doctoral research from all directions.

I also want to thank our Assistant Professor Seok Kang, who also gave me a lot of help. During my Ph.D, he gave me a lot of help in life and study.

I also want to thank the other members in our laboratory for their help in studying and living. As an international student in Japan, it is really lucky to get help from them.

In the doctoral program, we conducted research together and learned from a lot each other.

Finally, I want to thank my family. My parents have supported me mentally throughout my writing of this thesis and throughout my life.

Research achievements

Journals

- Lingjie Wei and Yuji Sakamoto, “Fast calculation method with foveated rendering for computer-generated holograms using an angle-changeable ray-tracing method,” Applied Optics, Vol. 58, Issue 5, pp. A258-A266 (2019).
- Lingjie Wei, Fumio Okuyama, Yuji Sakamoto, “Fast Calculation Method with Saccade Suppression for Computer-Generated Hologram based on Fresnel Zone Plate Limitation,” Optics Express. Vol. 28, Issue 9, pp. 13368-13383 (2020).

International conferences

- Lingjie Wei, Yuji Sakamoto, “A Fast Animation Generation System for Computer-Generated Hologram Using Ray-Tracing Method,” International Workshop on Advanced Image Technology 2018, F2-3, Jan. 2018
- Lingjie Wei, Yuji Sakamoto, “Fast calculation method with foveated rendering

matching human eye acuity for CGH head-mounted displays using angle-changeable ray tracing method," International Workshop on Holography and related technologies (IWH2018), SaO4, p64, Suzhou, China (November 30 to December 2, 2018).

- Lingjie Wei, Fumio Okuyama, Yuji Sakamoto, "Fast Calculation Method for Computer-Generated Holograms Using Saccade Suppression by Lowering the Resolution Based on Fresnel Zone Plate Reduction," International Display Workshops (IDW2019), 3DSA/3D9, Sapporo, Japan.

References

[1] C. M. Martin., "The impact of technology in the printed arts," *Washington University*, 2017.

[2] Lester. and Georgina., "Different jobs and responsibilities of various people involved in creating a website," *Arts Wales UK*, 2012.

[3] Sito. and Tom., "Moving innovation: A history of computer animation," *Massachusetts: MIT Press*, 2013.

[4] Mahoney. N. and Oikonomou. A., "Stereoscopic 3d in video games: A review of current design practices and challenges," *Computer Games (CGAMES), 2011 16th International Conference on. IEEE*, pp. 148–155, 2011.

[5] K. Wittlief., "Stereoscopic 3d film and animation – getting it right," *ACM SIGGRAPH*, 2009.

[6] R. Rickitt., "Special effects: The history and technique," *Billboard Books; 2nd edition*, 2007.

[7] F. Brooks., "What's real about virtual reality?," *IEEE Computer Graphics and Applications*, pp. 16–27, 1999.

[8] B. Atta., F. David., K. Ali., and A. Adedayo., "Accessibility-by-design: A framework for delivery-context-aware personalised media content re-purposing. hci and usability for e-inclusion," *Lecture Notes in Computer Science. Springer, Berlin, Heidelberg*, pp. 209–226, 2009.

[9] D. Sharp., "Monica pidgeon: Influential editor of 'architectural design' for more than 30 years," *The Independent*, 2009.

[10] J. Reedy. and S. Lunzman., "Model based design accelerates the development of mechanical locomotive controls," *SAE 2010 Commercial Vehicle Engineering Congress*, 2010.

[11] University of Leeds ISS., "What are computer graphics?," *Wayback Machine*, 2002.

[12] Z. Ray., "3-d filmmakers: Conversations with creators of stereoscopic motion pictures," *Scarecrow Press*, 2005.

[13] C. Matt., "Real d 3d theatrical system," *European Digital Cinema Forum*, 2017.

[14] T. L. Turner. and R. F. Hellbaum., "Lc shutter glasses provide 3-d display for simulated flight," *Information Display Magazine*, 1986.

[15] H. Michael., "Diffraction gratings," *Techniques of Physics. 6. Academic Press*, 1982.

[16] J. Mo., "Ophthalmic lenses and dispensing," *Elsevier Health Sciences*, 2003.

[17] D. Fattal., Z. Peng., T. Tran., S. Vo., M. Fiorentino., J. Brug., and R. G. Beausoleil., "A multi-directional backlight for a wide-angle, glasses-free three-dimensional display," *Nature*, 2013.

[18] D. Gabor., "A new microscopic principle," *Nature*, vol. 161, pp. 777–778, 1948.

[19] B. Guenter., S. Drucker., D. Tan., and J. Snyder., "Foveated 3d graphic," *Microsoft Research*, November 20, 2012.

[20] Sensics., "Understanding foveated rendering," *Medium. 2016–04–11*, pp. 57–64, Retrieved 2017-02-04.

[21] A. T. Bahill., M. R. Clark., and L. Stark., "The main sequence, a tool for studying human eye movements," *Mathematical Biosciences 24*, pp. 3–4, 1975.

[22] D. J. DeBitetto., "Holographic panoramic stereograms synthesized from white lightrecordings," *Appl. Opt. 8*, pp. 1740–1741, 1969.

[23] M. C. King., A. M. Noll., and D. H. Berry., "A new approach to computer generated holography," *Appl.Opt. 9*, pp. 9471–9475, 1970.

[24] K. Matsushima. and S. Nakahara., "Extremely high-definition full-parallax computer-generated hologram created by the polygon-based method," *Appl. Opt. 48*, pp. H54–H63, 2009.

[25] D. Arai., T. Shimobaba., K. Murano., Y. Endo., R. Hirayama., D. Hiyama., T. Kakue., and T. Ito., "Acceleration of computer-generated holograms using tilted wavefront recording plane method," *Optics express*, pp. 1740–1747, 2015.

[26] S. Jiao., Z. Zhuang., and W. Zou., "Fast computer generated hologram calculation with a mini look-up table incorporated with radial symmetric interpolation," *Optics express*, pp. 112–123, 2017.

[27] J. P. Waters., "Holographic image synthesis utilizing theoretical," *Appl. Phys. Lett. 9*, pp. 405–407, 1966.

[28] A. Appel., "Some techniques for machine rendering of solids," *AFIPS Joint Computer Conference*, pp. 37–45, 1968.

[29] T. Whitted., "An improved illumination model for shaded display," *Comm.ACM.23*, pp. 343–349, 1980.

[30] G. R. Hofmann., "Who invented ray tracing?," *The Visual Computer*, pp. 120–124, 1990.

[31] T. Ichikawa., T. Yoneyama., and Y. Sakamoto., "CGH calculation with the ray tracing method for the fourier transform optical system," *Optics Express*, pp. 32019–32031, 2013.

[32] T. Yoneyama., C. Yang., Y. Sakamoto., and F. Okuyama., "Eyepiece-type full-color electro-holographic display for binocular vision," *Proc. SPIE, 8644-38*, 2013.

[33] E. Murakami., Y. Oguro., and Y. Sakamoto., "Study on compact head-mounted display system using electro-holography for augmented reality," *IEICE Transactions on Electronics*, vol. E100.C, no. 11, pp. 965–971, 2017.

[34] T. Yoneyama., E. Murakami., Y. Oguro., H. Kubo., K. Yamaguchi., and Y. Sakamoto., "Holographic head-mounted display with correct accommodation and vergence stimuli," *Optical Engineering 57(6)*, p. 061619, 30 May 2018.

[35] M. Andrew., G. Andreas., and J. S. Kollin., "Holographic near-eye displays for virtual and augmented reality," *ACM Trans. Graph.*, vol. 36, pp. 85:1–85:16, July 2017.

[36] G. W. Stroke., "Lensless fourier-transform method for optical holography," *Appl. Phys. Lett.*, vol. 6, pp. 201–203, 1965.

[37] A. T. Duchowski., "A breadth-first survey of eye tracking applications," *Behavior Research Methods, Instruments, and Computers 34, 455-70*, 2002.

[38] R. Radach., J. Hyona., and H. Deubel., "The mind's eye: Cognitive and applied aspects of eye movement research," *North-Holland*, 2003.

[39] E. M. Reingold., L. C. Loschky., G. W. McConkie., and D. M. Stampe., "Gaze-contingent multiresolution displays: an integrative review," *Human Factors 45, 2, 307-28*, 2003.

[40] A. T. Duchkwski. and A. Çöltekin., "Foveated gazeconingent displays for periperal LOD management, 3D visualization, and stereo imaging," *ACM Trans. on Multimedia, Communications and Applications*, 2007.

[41] P. Baudisch., D. DeCarlo., A. T. Duchowski., and W. S. Geisler., "Focusing on the essential: considering attention in display design," *Commun. ACM 46*, pp. 60–66, 2003.

[42] B. Watson., N. Walker., L. F. Hodges., and A. Worden., "Managing level of detail through peripheral degradation: effects on search performance with a head-mounted display," *ACM Trans. Comput.-Hum. Interact. 4*, pp. 323–346, 1997.

[43] B. Watson., N. Walker., and L. F. Hodges., "Suprathreshold control of peripheral LOD," *ACM Trans. Graph. 23*, pp. 750–759, 2004.

[44] P. E. Ludwig., M. Motlagh., and C. N. Czyz., "Physiology, eye," *Treasure Island (FL): StatPearls Publishing*, 2020.

[45] H. Strasburger., I. Rentschler., and M. Jüttern., "Peripheral vision and pattern recognition: a review," *Journal of Vision*, December 2011.

[46] S. Kazempourradi., B. Soner., E. Ulusoy., and H. Ü1rey., "Full-color foveated three-dimensional holographic near-to-eye display," *ISDH 2018*, June 2018.

[47] J. Hong., Y. Kim., S. Hong., C. Shin., and H. Kang., "Gaze contingent hologram synthesis for holographic head-mounted display," *SPIE*, 2016.

[48] E. Moon., M. Kim., J. Roh., H. Kim., and J. Hahn., "Holographic head-mounted display with rgb light emitting diode light source," *Optics Express*, pp. 6526–6534, 2014.

[49] Gibson. and H. Lou., "Close-up photography and photomacrography," *2nd combined ed. Kodak Publication No. N-16. Rochester, NY: Eastman Kodak Company, Vol II: Photomacrography*, 1975.

[50] D. C. V. Essen. and C. H. Anderson., "Information processing strategies and pathways in the primate visual system," *An Introduction to Neural and Electronic Networks, 2nd ed*, pp. 45–76, 1995.

[51] Q. Sun., A. Patney., L.-Y. Wei., O. Shapira., J. Lu., P. Asente., S. Zhu., M. McGuire., D. Luebke., and A. Kaufman., "Towards virtual reality infinite walking: Dynamic saccadic redirection," *ACM Transactions on Graphics (Proceedings of SIGGRAPH)*, 2018.

[52] Carpenter. and Roger. H. S., "Movement of the eyes," *Pion Ltd; Subsequent*, pp. 70–71, 1988.

[53] R. H. Y. Chen. and T. D. Wilkinson, "Computer generated hologram with geometric occlusion using gpu-accelerated depth buffer rasterization for three-dimensional display," *Applied Optics*, pp. 4246–4255, 2009.

[54] L. Wei. and Y. Sakamoto., "Fast calculation method with foveated rendering for computer-generated holograms using an angle-changeable ray-tracing method," *Applied Optics*, pp. A258–A266, 2019.

[55] L. Wei. and Y. Sakamoto., "Fast calculation method with foveated rendering matching human eye acuity for cgh head-mounted displays using angle-changeable ray tracing method," *IWH2018, SaO4, p64, Suzhou, China*, 2018.